AN INSTITIÚID UM THAIGHDE EACNAMAÍOCHTA AGUS SÓISIALTA
ESRI ECONOMIC & SOCIAL RESEARCH INSTITUTE

ESRI Working Paper No. 771

February 2024

Keeping our heads above water: Spatially heterogeneous social vulnerabilities and climate adaptation*

Stefano Ceolotto & Niall Farrell

Climate change is among the biggest challenges of our time. Climate impacts and socioeconomic vulnerability are spatially heterogeneous. Hence, adaptation policies are more effective when designed at lower administrative levels. However, spatially-detailed social vulnerability profiles are often not available. This paper employs a Conditional Monte Carlo simulation-based methodology to generate social vulnerability profiles representative at the electoral division level. These are used to investigate climate risk, considering flood risk in Ireland as a case study. The results highlight that while population exposure offers insight into flood risk patterns, incorporating socioeconomic vulnerability allows a more precise identification of areas of priority.

Keywords. Flood risk, Socioeconomic vulnerability, Small area estimation, Electoral divisions, Climate change, Ireland

JEL Codes. C63, Q54, R11, Y91

* S. Ceolotto (corresponding author; stefano.ceolotto@cmcc.it), Euro-Mediterranean Center on Climate Change and Ca' Foscari University of Venice; N. Farrell (Niall.Farrell@esri.ie), The Economic and Social Research Institute and Trinity College Dublin.

1 Introduction

Socially vulnerable groups are often more severely affected by climate change and are less capable to put in place measures to reduce or transfer risk (Schelling, 1992; Baer, 2009; Cummins and Mahul, 2009; Hallegatte and Rozenberg, 2017; Rao et al., 2017; Park et al., 2018; Sánchez, 2018; IPCC, 2022). For example, lower-income households face affordability issues to purchase insurance coverage against (disastrous) climatic events (Barnett et al., 2008), a trend which is expected to be aggravated by climate change (Hudson et al., 2016; Hudson, 2018; Tesselaar et al., 2020). While mitigation efforts to keep global warming within 1.5°C above pre-industrial levels are considered the best option to limit damages from climate change (UNEP, 2021), halting greenhouse gas emissions would not prevent the climate impacts that are already occurring (EC, 2021). Therefore, adaptation measures are recognized as key tools to combat climate change (UNFCCC, 2015) thanks to their ability to reduce risk and generate "triple dividends" (Tanner et al., 2015; GCA, 2019).

Effective climate adaptation policies require a good understanding of climate impacts and of the characteristics of the social fabric, both of which are spatially heterogeneous. However, data and methodological limitations restrict the ability to estimate the spatial distribution of climate impacts and socioeconomic vulnerability. On one hand, socioeconomic data is often not available with a high level of spatial detail, and less granular data sources are used instead (Hallegatte et al., 2016; Hallegatte and Rozenberg, 2017; Rao et al., 2017; Breil et al., 2021). On the other hand, small area estimation is often subject to a number of distributional requirements that limit application (Farrell, 2023).

This paper demonstrates how a novel small area estimation technique can be used to overcome these limitations. This is applied to the evaluation of climate risk, using an Irish case study. Specifically, we combine a nationally representative survey of private households, containing rich profiles of economic and living conditions, with census data to estimate otherwise unavailable small area socioeconomic vulnerability profiles representative at the electoral division level. These estimates are subsequently interacted with spatial profiles of flood hazard across electoral divisions to assess the spatial variation of climate risk.

Our study provides two main contributions. First, it represents the first large-scale investigation of the spatial coincidence of potential climate shocks and socioeconomic vulnerability with a high level of spatial detail. Previous studies either rely on more crude socioeconomic measurements representative at the national or macroregional level (Kazama et al., 2009; Ronco et al., 2014; Winsemius et al., 2018; Park et al., 2018), or focus on smaller case studies at the city scale (Escuder-Bueno et al., 2012; Zhou et al., 2012; Sperotto et al., 2016; Szewrański et al., 2018; Sanchez-Guevara et al., 2019). Conducting a large-scale investigation of climate risk with a high level of spatial detail is important for multiple reasons. Using spatially-aggregated socioeconomic information can lead to aggregation bias, an underestimation of welfare losses and a potential mis-targeting of adaptation interventions (Sovacool et al., 2015). Moreover, since the effects of adaptation interventions can spill over across locations (Breil et al., 2021), governments and public administrations must have access to a detailed and comprehensive mapping of risk. Second, it employs a novel methodology to obtain robust and meaningful estimations of social vulnerability profiles. Small area estimation techniques allow researchers to produce estimates of socioeconomic information at the desired spatial level when primary data collection is precluded (Elbers et al., 2003; Tarozzi and Deaton, 2009; Molina and Rao, 2010; Salvati et al., 2010; O'Donoghue et al., 2013). However, they often rely on restrictive distributional assumptions, which can lead to biased estimates if violated. We overcome this limitation by adopting a Conditional Monte Carlo (CMC) simulation-based methodology, developed by (Farrell, 2023), that

generates small area estimates of socioeconomic characteristics without relying on restrictive assumptions. Crucially, this provides a standardised, comparable framework for socioeconomic impact estimation, which can be applied across many jurisdictions and policy priorities. This also represents a novel application of small area estimation techniques, which have mainly been utilised to investigate regional development and to simulate the effects of socioeconomic shocks. Previous environmental applications include the distributional impacts of agro-environmental policies (Hynes et al., 2009), quantifying travel costs and economic values of environmental amenities visits (Cullinan, 2011), estimating changes in commuting costs due to climate shocks (Kilgarriff et al., 2019), and assessing the incidence of carbon taxation (Chan and Sayre, Forthcoming). This is the first application to investigate the co-incidence of climate and socioeconomic vulnerabilities.

Ireland provides an appropriate context of analysis. There is a rich set of climatic, demographic and socioeconomic data that facilitate the analysis. In addition, Ireland is experiencing effects of climate change on natural and human systems comparable to those observed in other countries (Desmond et al., 2017). Therefore, the findings of this study can inform both Irish and international policy decision-making.

Flooding is often regarded as the natural hazard with the highest impact on society, having the highest number of events and affected people worldwide and the second highest economic losses (CRED-UNDRR, 2020). In Europe, floods account for over 45% of the €560 billion total economic losses in the period 1980-2021 (EEA, 2023). Climate change is projected to increase the risk of and damage from flooding events, both worldwide (Madsen et al., 2013; Vousdoukas et al., 2018; Willner et al., 2018) and in Ireland (Desmond et al., 2017; Nolan and Flanagan, 2020; Ryan et al., 2021). The combination of these factors thus makes flood risk a particularly sensible topic to analyse.

The analysis employs a stepwise approach to elicit the contribution that each additional source of information — i.e. climate impacts, population exposure and socioeconomic vulnerability of this population — provides when identifying hot spots of vulnerability. We first consider climate impacts alone. We elicit the percentage of an electoral division's surface area affected by flooding events. We define this metric as 'flood hazard'. Second, we evaluate population 'exposure' by considering the percentage of the population in an electoral division exposed to flooding. Finally, we incorporate the small area estimates of socioeconomic vulnerability. We define this metric as 'flood risk'. We choose "at risk of poverty" (AROP) as a measure of socioeconomic vulnerability. This is intended to control for limitations in self-protection from climate impacts: people with worse financial conditions might lack sufficient resources to autonomously put in place measures to protect themselves or adapt to shocks. We follow the Eurostat definition, which classifies a household as being at risk of poverty if its annual equivalised disposable income falls below the 60% of the national median annual equivalised disposable income. We employ a hot spots analysis to identify clusters of high vulnerability for each of the measures considered. Such an approach allows us to: (i) provide a multi-dimensional picture of the most affected and vulnerable areas; and, (ii) evaluate how climate adaptation and protection priorities change across indicators. This will help policymakers to better target adaptation interventions based on their views of justice and equity as well as the policy goals they aim to achieve.

The identified hot spots change substantially moving from flood hazard (climate impacts alone) to flood exposure (coincidence of climate impacts and population exposure). There is less variation in hot spots identification when moving from flood exposure to flood risk (coincidence of climate impacts, population exposure and socioeconomic vulnerability) is investigated. The incorporation of socioeconomic vulnerability does, however, allow for hot spots of vulnerability to be prioritised in policy decision-making. Considering

different redistribution preferences in the computation of flood risk narrows the focus on those previously identified. We conclude that the quantification of flood exposure provides a first-round approximation of locations which may require adaptation interventions. Adding metrics of social vulnerability identifies locations of highest priority given the societal preferences towards equity.

The remainder of the paper is structured as follows. Section 2 describes the main datasets used in the analysis. Section 3 discusses the small area estimation technique and the methodology to combine the social vulnerability measures thus generated with flood maps to obtain indicators of flood risk at the electoral division level. Section 4 presents the results of the flood vulnerability analysis. Finally, Section 5 concludes.

2 Data

To investigate climate and social vulnerability in Ireland at the electoral division level, we combine data on flood extents, demographic characteristics and socioeconomic characteristics. The aim is to consider the highest level of spatial disaggregation while retaining sufficient information and data quality. In this perspective, the limiting factor is represented by socioeconomic data. We choose electoral divisions as the units of analysis since they are the most spatially disaggregated datasource containing rich socioeconomic data.[1]

The Central Statistics Office (CSO) defines electoral divisions (EDs) as the smallest legally defined administrative areas in Ireland. There are originally 3,440 EDs. However, 32 scarcely populated EDs have been amalgamated into neighbouring ones for reasons of confidentiality, leaving a final count of 3,409 EDs for statistical and analytical purposes.

The demographic and socioeconomic data are considered for the year 2016. Demographic information is taken from the Census and socioeconomic information comes from the European Union Survey of Income and Living Conditions (EU-SILC). While the SILC is available up until 2021, the most recent Census for which full results were available at the time of the study is 2016, which determines our choice of year of analysis.[2]

2.1 Flood data

The flood data is provided by the Irish Office of Public Works (OPW) national flood information portal. We use the 'catchment flood risk assessment management' (CFRAM) flood maps, which report areas that are predicted to be inundated during a theoretical or "design" flood event based on an estimated probability of occurrence and climate change scenario. Flooding can come from three sources: coastal (i.e. sea and ocean), fluvial (i.e. rivers and estuaries) and pluvial (i.e. rainfall). The latter, however, is only available for a few, selected locations and for one climate change scenario,[3] hence it has not been used in the analysis presented here.

The probability of occurrence is defined in terms of 'annual exceedance probability' (AEP), representing the probability that a flooding event of a certain magnitude, or more severe, occurs in any given year. Events are divided into three classes. High probability events, with an AEP $= 10\%$, are less severe events. Medium

[1] More spatially disaggregated data exist, known as small areas (SA), but they do not present as rich a set of socioeconomic information.

[2] Another Census was conducted in 2022. However only a few preliminary results have been published, which prevents us from using it in the analysis. Information on the 2016 Census can be found at: https://www.cso.ie/en/census/census2016reports/.

[3] The locations are Raphoe in County Donegal, and Dublin City. Climate change is assessed under the 'current scenario'.

probability events are characterised by AEP = 1% for fluvial flooding and AEP = 0.5% for coastal flooding. Low probability events are more rare and more severe events, and present an AEP = 0.1%. In addition, maps are developed for three climate change scenarios: in order of severity, current scenario, medium-range future scenario and high-end future scenario. The analysis presented below is based on low probability events under a high-end climate change scenario to offer a representation of a worst-case scenario.[4]

OPW prepares three types of CFRAM maps: flood extent maps, flood depth maps and flood risk maps. Flood extent maps report the estimated extents, peak water levels and flows of floods, taking into account the geographical and morphological characteristics of the territory, including existing flood defences. Flood depth maps indicate the maximum estimated depth of flooding at a given location. Flood risk maps contain information on the number of inhabitants, type of economic activities and protected areas at risk of flooding, in line with the guidelines reported in the Flood Directive (2007/60/EC). Unfortunately, flood depth and flood risk maps are not available for the entire country in the required format for our spatial analysis. For this reason, the analysis presented below is based on flood extent maps, which are the only ones available nation-wide in vector format.

Climate risk is assumed to originate from a combination of hazard, exposure and vulnerability or susceptibility (Field et al., 2012; Giupponi et al., 2015). Hazard relates to the climate event's parameters and intensity. Exposure relates to the elements at risk, or receptors, in the affected region. Vulnerability/susceptibility refers to the degree to which receptors can be affected by and are capable to cope with the climate event, based on topographical and socioeconomic characteristics (Ronco et al., 2014). Although flood extent maps are generated taking into consideration topographical elements (including the presence of buildings and infrastructures),[5] they do not contain information on the water depth and velocity, which are among the most relevant metrics to assess flood hazard (Citeau, 2003; DEFRA, 2006; Ronco et al., 2014). This means that the measure we derive represents an upper bound of flood hazard.

Figure 1 displays the coastal and fluvial CFRAM flood extents map for low probability events under a high-end climate change scenario. Fluvial flooding, represented with a light-blue shading on the map, interests primarily the course and estuaries of the Shannon river in central Ireland, of the Laune river in the south-west, of the Barrow river and Liffey river in the centre and east, and of the Lough Conn and Moy river in the north-west. Coastal flooding, represented with a darker blue shading, takes place on the eastern coast (affecting the cities of Dublin, Dundalk, Wicklow), along the south-east coast (Dungarvan, Tramore, Waterford, Wexford), and on the western coast (Castlemain, Limerick, Galway). One area that is notably missing is the city of Cork, the second largest urban area in Ireland. This is located in the south-western part of the country and is often affected by flooding events (Olbert et al., 2022). While CFRAM maps for current and medium-range future scenarios present flood extents for this area, they are not included for the high-end future scenario.[6]

[4] Other combinations of AEP and climate change scenarios are not reported for ease of presentation, but they are available from the authors upon request.

[5] The detailed description of the technical process for the development of OPW's flood maps can be found in the user guidelines (https://www.floodinfo.ie/map/general_map_user_guidance_notes/) and in the hydraulic and hydrological reports (https://www.floodinfo.ie/publications/?t=19&t=20).

[6] Upon consultation with OPW it emerged that data for the Cork area was part of the Lee Pilot CFRAM programme and that models were run for the high-end future scenario; nevertheless, it was not included in the high-end future scenario CFRAM maps.

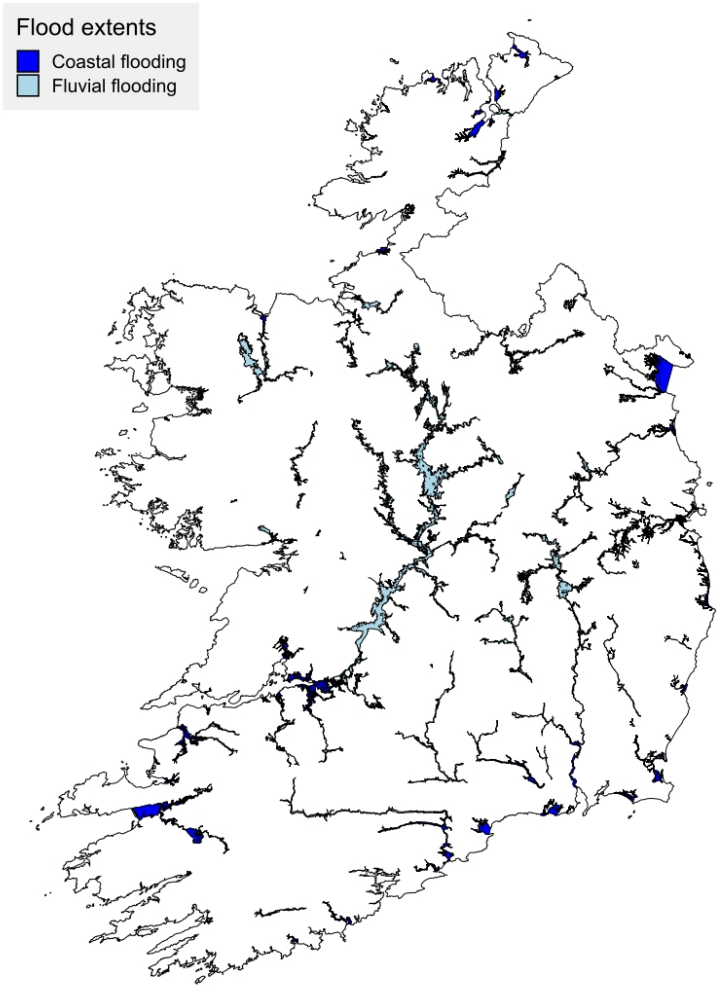

Figure 1: Flood extents map

2.2 Demographic and socioeconomic data

We first want to assess the exposure of the population to flooding. In order to do this, we need demographic data. Then, we wish to explore the additional insight provided by considering socioeconomic information, such as the distribution of inequality or vulnerability, when assessing the exposure in a given population. For this, spatially-referenced socioeconomic data is required.

This information is not readily available, however there are related datasets that provide subsets of said information. Demographic data presents demographic and socioeconomic indicators representative at a spatially disaggregated level. However, it does not allow the co-incidence of two or more of such indicators to be identified. Moreover, it typically does not provide insight on vulnerability profiles. For example, census data contains information on average incomes, but not on the number of households below the poverty line. On the other hand, survey microdata gives insight into the distribution of variables such as income and various dimensions of socioeconomic vulnerability. These datasets, however, are often nationally representative. Small area estimation techniques, by combining the power of both these datasources, allow researchers to conduct

a distributional analysis of vulnerability profiles at the desired level of spatial disaggregation.

2.2.1 Demographic data

To estimate the population in an electoral division affected by flooding, we use information on daytime population and workplace zones. This is collected by the CSO as part of the Census since 2011, and it provides population data for a 1km^2 grid of Ireland.[7] The procedure to assign population values to flooded areas is explained in Section 3.2. Figure 2 displays the population for the 1km^2 grid of Ireland, converted into raster format for presentation purposes. It can be seen that the majority of Ireland's territory is scarcely populated. The most highly populated area by far is the city of Dublin and its metropolitan area, in the east. Other relatively densely populated areas are the city of Cork in the south, and the cities of Limerick and Galway in the west.

The second demographic dataset that we use is the Small Area Population Statistics (SAPS), also produced by the CSO as part of the Census. In addition to the total number of inhabitants in each of the 3,409 electoral divisions, the SAPS contains information on 45 population statistics divided into 14 thematic areas. These include breakdonws of the population by age cohort, marital status, gender, nationality, ethnicity, religious beliefs, family composition, type and characteristics of accommodation, employment, working sector, education level, car and PC ownership and internet access.[8] This information is used for calibration in the small area estimation as explained in Section 3.3.

2.2.2 Socioeconomic data

The European Union Survey of Income and Living Conditions (EU-SILC) is a voluntary, nationally representative cross-sectional survey of private households in Ireland conducted by the CSO under EU legislation (Regulation (EC) 1177/2003). It contains over 200 questions to elicit information on, among others, household income, employment, economic status, educational attainment, health condition, ownership of car, PC and other home appliances, and to derive indicators on deprivation, poverty and social exclusion. We use the 2016 version accessed via the Irish Social Science Data Archive - www.ucd.ie/issda.

The SILC contains valuable information on socioeconomic characteristics that are required to derive accurate measures of social vulnerability and that are not included in census data. The survey is constructed to be representative of the national population, but it does not ensure representativeness for higher degrees of spatial disaggregation. Therefore, the information it provides is not directly applicable to an analysis at the electoral division level. This is made possible by the adoption of a small area estimation technique which, as discussed in Section 3.3, allows us to combine the rich information provided by the SILC with the distribution of demographic characteristics in each electoral division observed in the SAPS, so that social vulnerability measurements representative at the electoral division level can be obtained.

[7] Information and data are available at: https://www.cso.ie/en/census/census2016reports/workplacezonesand1kmpopulationgrids/

[8] Information on the SAPS and the thematic areas can be found at: https://www.cso.ie/en/census/census2016reports/census2016smallareapopulationstatistics/.

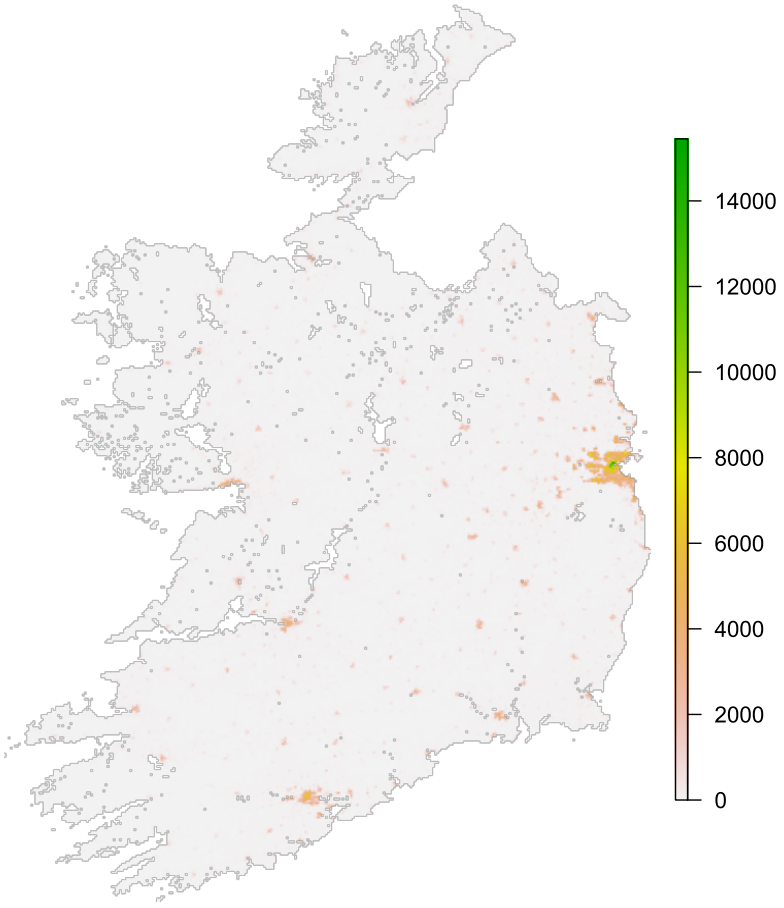

Figure 2: Total population aggregated into 1km^2 grid cells

3 Methods

After having collected all the relevant data, the task is then to: (i) assign flood values to electoral division, (ii) generate social vulnerability profiles representative at the electoral division level, (iii) bring the outcomes of these two steps together to quantify flood risk across electoral divisions. This section details the operations we implement in order to accomplish such tasks.

3.1 Flood hazard assessment

The OPW flood datasets are shapefiles in vector format with unique identifiers for each flood geometry. To assign flood extents to each electoral division, we first compute the spatial intersection between coastal and fluvial flood geometries and electoral division polygons. Since in some cases coastal and fluvial flood geometries present partial or full overlaps, we unify floods belonging to the same electoral division into a single spatial element to avoid double-counting.[9] We calculate the area of this unified geometry to derive the total area of an electoral division affected by flooding. Finally, flood hazard is given by the percentage of an

[9] In order to perform this operation, some flood geometries are removed due to their geometry type being invalid for said operation. The operation can be performed only with geometry types 'polygon', 'multipolygon' or their collection. Conversely, geometry types 'linestring', 'multilinestring' and their collection are not supported. For events with low probability under a high-end climate change scenario there is one flood geometry in the fluvial dataset containing elements of type 'multilinestring', which would cause the operation to fail. This geometry has been removed from the analysis.

electoral division's surface which is affected by flooding as expressed by the following formula:

$$Flood\ hazard_i = \frac{Total\ area\ affected\ by flooding_i}{Total\ electoral\ division\ area_i}, \text{with } i \in I \tag{1}$$

where $I \subset N$ is the subset of all electoral divisions that are intersected by at least one flood geometry, N being the set of all Irish electoral divisions. Electoral divisions that are not intersected by any flood geometries are assigned a value of flood hazard equal to 0. For those electoral division belonging to I, the percentage of area affected by flooding has a right skewed distribution with a minimum of 0.00002%, a maximum of 98.95% and an average of 10.69%.

To allow for the comparability of different metrics and maps, the flood hazard measure presented in Equation 1 is normalised and converted into an index ranging from 0 (no hazard) to 1 (highest hazard in the case study area, Zabeo et al., 2011; Ronco et al., 2014; Sperotto et al., 2016). This is done by rescaling the flood hazard in each electoral division relative to the electoral division with the highest hazard value:

$$H_n = \frac{Flood\ hazard_n}{\max(Flood\ hazard)}, \text{ with } n \in N. \tag{2}$$

3.2 Flood exposure assessment

To estimate the population in each electoral division affected by flooding we start by deriving the spatial intersection between the unified flood geometries previously generated, each of which relates to a single electoral division, and the 1km^2 grid mentioned in Section 2.2.1. Essentially, a flood geometry belonging to electoral division $i \in I$, F_i, is partitioned into K sub-geometries, $F_{(i,k)}$,[10] each associated to one of the K 1km^2 grid cells intersecting F_i. We compute the areas of each sub-geometry $F_{(i,k)}$, and then we derive the percentage of grid cell k's area that is covered by the flood sub-geometry $F_{(i,k)}$ as the ratio between the area of $F_{(i,k)}$ and the area of the grid cell[11]. Assuming equal distribution of the population within a grid cell, we can say that this also corresponds to the percentage of grid cell k's population that is affected by the flood sub-geometry $F_{(i,k)}$. This is then multiplied by the population of grid cell k to get the number of individuals affected by the flood sub-geometry $F_{(i,k)}$. The sum of all K sub-geometries gives the total number of individuals affected by flood geometry F_i, which corresponds to the total population in electoral division i at risk of flooding:

$$\begin{aligned} Total\ population\ at\ risk\ of\ flooding_i = \sum_{k=1}^{K} & Percentage\ of\ grid\ cell\ k's\ population\ affected\ by\ F_{(i,k)} \\ & \times Grid\ cell\ population_k, \text{ with } i \in I \end{aligned} \tag{3}$$

Finally, flood exposure is given by the percentage of an electoral division's population affected by flooding as follows:

$$Flood\ exposure_i = \frac{Total\ population\ affected\ by\ flooding_i}{Total\ electoral\ division\ population_i}, \text{ with } i \in I. \tag{4}$$

Electoral divisions that are not intersected by any flood geometries are assigned a value of flood exposure

[10] Such that $F_{(i,k)} \subset F_i$ and $F_{(i,k)} \neq \emptyset, \forall k \in K$; $F_{(i,k)} \cap F_{(i,l)} = \emptyset$ for $k \neq l, k, l \in K$; $F_{(i,1)} \cup \cdots \cup F_{(i,k)} \cup \ldots F_{(i,K)} = F_{(i)}$.

[11] Since the grid cell polygons do include not rivers, lakes or other water bodies, and they follow the shape of the coastline, not all grid cells have an area of exactly 1km^2.

equal to 0. Similarly to flood hazard, for electoral divisions belonging to I the percentage of population affected by flooding is positively skewed, with a minimum of 0.0004%, a maximum of 100.00% and an average of 9.55%. Since this measure of flood exposure is derived from the extension of the flooded area in each electoral division, it also contains flood hazard information.

The assumption of uniform distribution is a strong one. However, without information on the distribution of dwellings within grid cells, the procedure discussed above represents the best the data at our disposal allows. Nevertheless, we can assess the performance of the procedure by using it to estimate the electoral divisions' population and compare the result to the values reported in the census. Specifically, we test the correlation between the total population in each electoral division obtained with our spatial analysis and the actual population reported in the census. The resulting correlation coefficient is 0.984 , which is significant at the 99% level. Hence, we reject the null hypothesis of no correlation, and we can say that there is a strong positive correlation between the two measures. This is also shown by Figure 3, which displays a scatter plot of the estimated population against the census values. The data presents a clear linear trend, very close to the 90° line of perfect linear relation. Overall, this suggests that the spatial procedure we employ performs well in approximating total population across electoral divisions, and is therefore reassuring in terms of the potential distortions generated in estimating flood exposure.

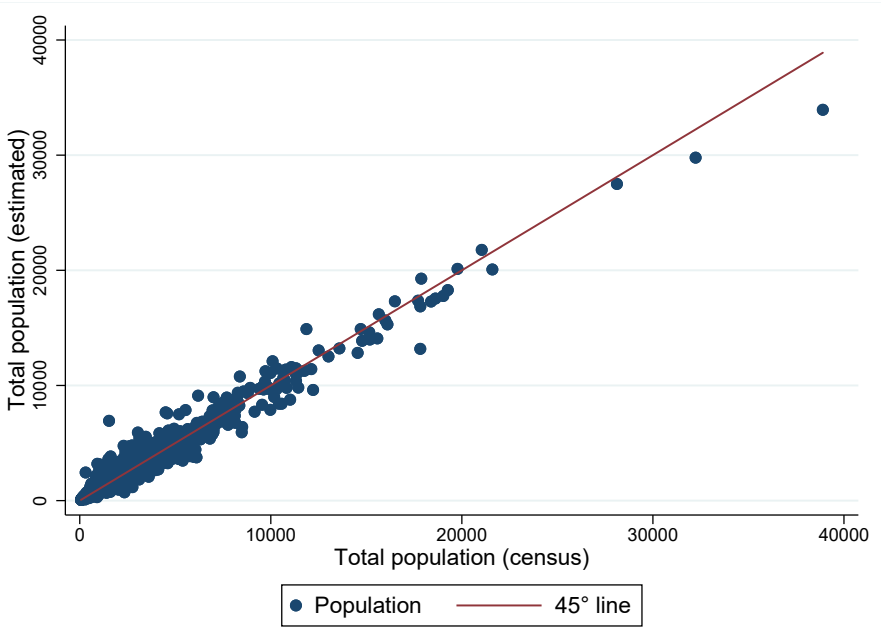

Figure 3: Total electoral division population: estimated vs census

Notes. This graph displays a scatter plot of the total population in each electoral divisions estimated with spatial operations (on the vertical axis) against that provided in the 2016 census (horizontal axis). It also reports the 45° line, which corresponds to a one-to-one relation.

There are eight cases in which the estimated population affected by flooding exceeds the total electoral division's population. These are all relatively scarcely populated electoral divisions neighboring with more populous ones, with flooding either covering a substantial part of their surface or being located on their borders with more populous electoral divisions, and with one or more grid cells intersecting the flooded area also overlaying more populous electoral divisions. Hence, the spatial analysis is picking up individuals

residing in other places and assigning them to the flooded areas, thus overestimating the population affected by flooding. The corresponding values of flood exposure range from 1.009 to 1.421. For these electoral divisions, we have decided to replace flood exposure with 1 if at least 90% of the electoral division's area is affected by flooding (i.e. $Flood\ hazard \geqslant 0.9$),[12]. Conversely, if $Flood\ hazard < 0.9$, the electoral division is removed from the analysis and flood exposure is coded as missing. This results in four electoral divisions being removed.[13]

Finally, flood exposure is normalised and converted into an index ranging from 0 (no exposure) to 1 (highest exposure in the case study area) by rescaling the flood exposure in each electoral division relative to the electoral division with the highest exposure value:

$$E_n = \frac{Flood\ exposure_n}{\max(Flood\ exposure)}, \text{ with } n \in N. \tag{5}$$

3.3 Small area estimation of social vulnerability

Small area estimates of poverty and inequality are required to effectively target economic and social policy towards vulnerable populations, including climate adaptation policy. The importance of reliable spatial estimates will grow with trends of increasing global inequality and, indeed, the growing influence of spatially-heterogeneous climate-related welfare shocks. As Hallegatte and Rozenberg (2017) discuss, spatially-refined poverty data will be required to target climate policy towards the microregions and socioeconomic groups that are most negatively affected. Poverty data at the small area level are not readily available in many contexts as survey microdata are often designed to be representative at the national or aggregated regional level. We use a small area estimation procedure known as Conditional Monte Carlo (CMC) to overcome this limitation. While small area estimates and spatial microsimulation methods have been used in a wide range of applications, they have yet to be applied in the context of climate vulnerability assessment at a national scale. The general procedure, described in greater detail by Farrell (2023), combines the micro-level power of survey data with the spatial information of census data.

In Ireland, the closest data source is that of the Pobal HP Deprivation Index[14], which relies on spatial data primarily sourced from the census. A number of indicators including population change, age dependency, spatial profession profiles, unemployment rates, education levels and housing demographics are used to construct a composite index of deprivation. While providing a useful indicator as to deprivation rates at the small area level, this index does not feature income, or similar income and social welfare-related variables present in survey data. The small area estimation procedure employed in this paper provides this contribution.

The estimation procedure takes the following form. The objective is to estimate the expected value of a variable of interest, H_i, which details the small area distribution of an outcome variable x for small area i in region R, where $i \subset R$. Defining l_i as the estimator, this may be characterised as:

$$l_i = E[H_i(x_i)] \tag{6}$$

[12] From which the maximum of 100% of population affected by flooding reported above. Without them, the maximum percentage of an electoral division's population at risk of flooding is 99.57%.

[13] The electoral divisions removed from the analysis are Cappavilla (Co. Clare), Lough Atalia (Co. Galway), Mansion House A (Co. Dublin) and North Dock B (Co. Dublin).

[14] See https://www.pobal.ie/pobal-hp-deprivation-index/

Assume there is a random vector y_i taking finite values in $\{i = 1, ..., N\}$. The y_i vector is correlated with x_i. Using conditional expectations, we can transform the l_i estimator to the expected value for H_i, conditional on the observed distribution of covariates y_i:

$$l_i = E[H_i(x_i)|Y = y_i]. \tag{7}$$

Then, l_i may be estimated using Monte Carlo sampling, with J replications, as:

$$l_i = E\Bigg[H_i(x_i)|Y = y\Bigg] = \frac{1}{J}\sum_{j}^{J}\Bigg[H_{i,j}(x_i)|Y = y_i\Bigg] \tag{8}$$

where $H_{i,j}(x_i)$ is the j^{th} Monte Carlo replication for ED i.

Each Monte Carlo replication is a sample of households drawn from region R such that we obtain an estimate of the statistical moment of interest, $H_i(x_i)$. As $H_i(x_i)$ is calculated conditional on the known distribution of y_i covariates, the sample of households drawn from region R must be chosen such that the the Y distribution of covariates corresponds to the known y_i distribution. A rejection sampling procedure is employed to calculate each Monte Carlo replication. Rejection sampling involves sampling a number of observations (e.g. households) from a microdata population R such that the distribution of Y covariates for sampled households corresponds to the known y_i distribution (i.e. $Y = y_i$).

The rejection sampling procedure draws on the quota sampling methodology developed by Farrell et al. (2013) and O'Donoghue et al. (2013). The algorithm operates by consecutively sampling households. As the algorithm assigns households, concurrent counts for the vector of Y covariates are noted. Households that violate the distribution of relevant covariates are removed from the candidate sample. To illustrate, the y_i vector may specify a particular distribution of pensioners for small area i. If this value is zero, or the y_i allocation has been fulfilled by the algorithm, all households containing pensioners are removed from the candidate sample. The sampling procedure does not replace households that have already been assigned to small area i, improving efficiency relative to other combinatorial optimisation algorithms such as simulated annealing and facilitating the CMC procedure. As the algorithm approaches convergence with the census totals for small area i, however, it may be infeasible to meet all remaining quotas for the y_i distribution of covariates, given the intra-household distribution contained within the microdata. For instance, we may be controlling for occupation and education status, with the final household requiring a scientist without a third level qualification. This may not be present in the dataset. A secondary set of less restrictive constraints is then called upon, such that the required number of households are assigned. While this introduces some additional noise into the estimate, under the assumption that the households assigned under the secondary set of constraints are randomly allocated, this does not bias the procedure, as demonstrated by Farrell (2023). For each small area i, microdata are sampled from the SILC survey dataset such that the distribution of census predictors for sampled households corresponds to the distribution of covariates observed in the SAPS census data, where $J = 100$. Table 1 reports the variables that constitute the primary and secondary sets of constraints. Households are allocated such that the distribution of income is centred around the median value reported by the Central Statistics Office. As households are allocated to the simulation population using the sequential process, a concurrent median is calculated. Should the concurrent median be greater than the CSO-stated median, households below the median are allocated in the subsequent iteration. The converse is true should the concurrent count exceed the median. When the primary set of constraints fails to

allocate the required number of households, the secondary set of constraints is called upon to allocate the remaining households. This is generally less than 5% of the total sample. The variables in the secondary set of constraints are selected because they explain the majority of the variation in ED-level income.

Table 1: Variables used in the rejection sampling procedure

Variable	Type	Values	Constraint
Majority of household income from welfare payments	Dichotomous	1 = Yes	Primary; Secondary
Majority of household income from statutory pension payments	Dichotomous	1 = Yes	Primary; Secondary
Median ED income	Continuous	€	Primary; Secondary
Household PC ownership	Dichotomous	1 = Yes	Primary
Household car ownership	Categorical	0–more than 4	Primary
Household internet access	Dichotomous	1 = Yes	Primary
Household tenure type	Categorical	Owner, renter, living rent-free	Primary
Household dwelling type	Categorical	House, flat/apartment/bedsit, other	Primary

3.4 Flood risk assessment

According to the Flood Directive (2007/60/EC), which represents the legislative framework to guide flood management in the European Union, flood risk originates by the combination of hazard, exposure and vulnerability. To produce a measure of flood risk in accordance with this definition, we reweigh flood exposure by some measure of social vulnerability. In relation to climate impacts, social vulnerability depends on factors that can drive or increase the level of risk (such as age or physical and mental health), on socioeconomic conditions that can limit the ability to react and adapt, and on morphological and infrastructural aspects that can exacerbate the consequences of an event (Parry et al., 2007; Lindley et al., 2011).

In our analysis, we focuse primarily on "at risk of poverty" (AROP) as a measure of social vulnerability. This is intended to control for limitations in self-protection from climate impacts: people with worse financial conditions might lack sufficient resources to autonomously put in place measures to protect themselves or adapt to shocks. We follow the Eurostat definition, which classifies a household as being at risk of poverty if its annual equivalised disposable income falls below the 60% of the national median annual equivalised disposable income.[15] The SILC contains a household-level indicator of being at risk of poverty. A corresponding measure representative at the electoral division level is estimated through the small area estimation technique. Finally, we compute the percentage of households in an electoral division who are at risk of poverty, which represents the measure of social vulnerability used throughout the analysis. Figure 4

[15]The Eurostat definition can be found at: https://ec.europa.eu/eurostat/statistics-explained/index.php?title=Glossary:At-risk-of-poverty_rate. This is also the definition adopted by the CSO. The CSO's computation procedure is outlined at: https://www.cso.ie/en/media/csoie/releasespublications/documents/ep/surveyonincomeandlivingconditions/2020/factsheets/At_Risk_of_Poverty_Explained.pdf.

shows the distribution of the percentage of households are at risk of poverty across Irish electoral divisions.

Yet, economic disadvantages are not the only way in which social vulnerability can exacerbate climate impacts. For example, physical or mental impairments can limit the ability to react to an event, thus increasing the level of risk even in the presence of protection measures. Hence, we replicate the analysis considering the percentage of households in an electoral division that derive the majority of their income from old-age pension (OAP), which is paid to individuals from the age of 66 who have enough (PRSI) contributions.[16] This, however, represents an imperfect measure of vulnerability since: (i) it does not give an exact indication of the age composition of these households; (ii) it conveys no information on the household's social network; and (iii) the state pension is paid even if households have other sources of income. Therefore, we also investigate the joint distribution of being at risk of poverty and deriving the majority of income from old-age pension, and, as a third social vulnerability measure, we consider the percentage of households in an electoral division that derive the majority of their income from old-age pension and are also at risk of poverty (OAP-AROP). These are individuals who are more physically vulnerable and also lack the capacity to put in place self-protection measures, thus being among the top priorities for climate risk adaptation interventions. The CSO provides information on on the proportion of households in an electoral division for whom state pension represents the majority of household income. In addition, the SILC contains household-level information on old-age benefits as well as an indicator of being at risk of poverty. These and their interaction are converted into percentages representative at the electoral division level through the small area estimation technique.

Following the literature on cost-benefit analysis of climate change (see, among others, Azar and Sterner, 1996; Fankhauser et al., 1997; Azar, 1999; Pearce, 2003), we compute social vulnerability weights as:

$$W_n = \left(\frac{\textit{Social vulnerability measure}_n}{\textit{Average percantage of households AROP}} \right)^e, \text{ with } n \in N, \tag{9}$$

where the denominator is the average for all Irish electoral divisions, and e can be interpreted as a measure of redistribution preferences or inequality aversion. Electoral divisions with a percentage of households at risk of poverty above the national average are assigned weights greater than 1, whereas electoral divisions with a percentage below the national average receive weights between 0 and 1.[17]

The bigger e the higher the weights assigned to more vulnerable electoral divisions and the lower the weights of less vulnerable ones. This should be determined empirically based on societal preferences for equity and justice (Anthoff et al., 2009). For instance, Rawlsian (Rawls, 1971) or Prioritarian (Broome, 1991) views of justice would call for values of $e > 1$, while Libertarian (Hayek, 1960) or Elitist (Nozick, 1974) views would prescribe values close to unity or even below. The literature typically sets e between 1 and 1.5 (Cline, 1992), although values as low as 0.8 or 0.5 have also been adopted (Pearce and Ulph, 1994; Fankhauser et al., 1997). Some have argued that the value of e can be inferred from taxation and foreign aid policies (Cowell and Gardiner, 1999) although many would be cautions in inferring ethical parameters from revealed social preferences (Anthoff et al., 2009). Therefore, absent an *a priori* knowledge on justice and redistribution

[16] Information on the Irish State Pension scheme can be found on the Citizen Information website: https://www.citizensinformation.ie/en/social_welfare/social_welfare_payments/older_and_retired_people/state_pension_contributory.html.

[17] Notice that most of the aforementioned papers compute social or equity weights based on income (Y). Their weights take the form $W_n = \left(\frac{\overline{Y}}{Y_n}\right)^{\sigma}$. Differently from income, our measures of social vulnerability have a negative connotation — i.e. the more the worse. Hence, to allow for more vulnerable electoral division to be given higher weights, we invert the order of numerator and denominator. This corresponds to $e = -\sigma$.

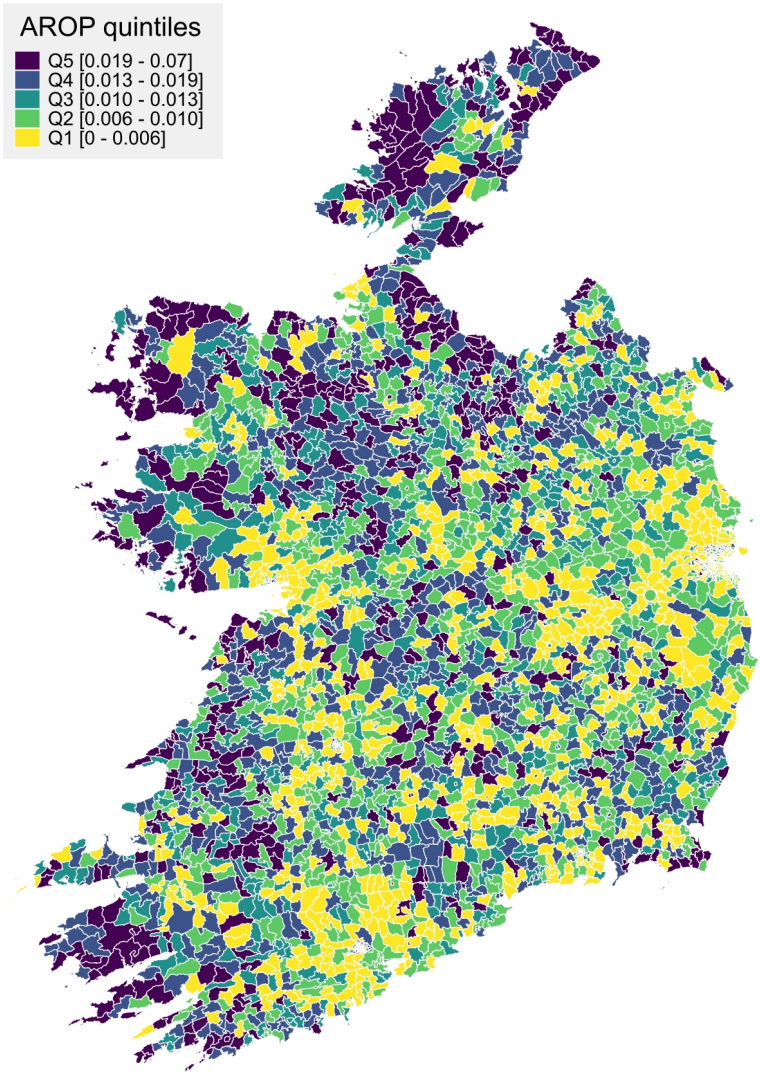

Figure 4: Percentage of households at risk of poverty

Notes. This graph displays the quintiles of the distribution of our social vulnerability measure, namely the percentage of households in an electoral division who are at risk of poverty. Poverty risk is given by the household's annual equivalised disposable income being below the 60% of the national median annual equivalised disposable income.

preferences in the specific context investigated, we decide to embrace simplicity and adopt $e = 1$ for most of the analysis.[18] We also test how different values affect our results.

Flood risk is obtained multiplying the flood exposure value of each electoral division by its corresponding social vulnerability weight:

$$\textit{Flood risk}_n = \textit{Flood exposure}_n \times W_n, \text{ with } n \in N. \tag{10}$$

Unlike the measures of flood hazard and flood exposure in Equations 1 and 4, respectively, flood risk is not bound between 0 and 1, but can range between $[0; +\infty)$. Also, its values do not have a direct interpretation.

Finally, we convert the flood risk measure into an index by dividing the flood risk in each electoral district

[18] This corresponds to Bernoulli-Nash-type weights (Fankhauser et al., 1997), where relative changes are given equal weight (Anthoff et al., 2009).

by the highest flood risk in the sample:

$$R_n = \frac{Flood\ risk_n}{\max(Flood\ risk)},\ \text{with } n \in N. \tag{11}$$

This now ranges from 0 (no risk) to 1 (highest risk) and takes a relative interpretation: what is the level of flood risk in a given electoral division proportional to the electoral division with the highest level of risk. Social vulnerability is represented by the percentage of households at risk of poverty.

3.5 Hot spots analysis

Although it is important to measure the degree of climate hazard, exposure and risk at the small area level, policies often target wider regions rather than individual electoral divisions. It is therefore equally important to investigate the spatial distribution of climate hazard, exposure and risk. For this reason, we conduct a hot spots analysis to identify the presence of clusters of high-hazard/exposure/risk administrative areas.

Hot and cold spots are based on the spatial autocorrelation of a certain parameter across geographic locations. They essentially represent groups of outliers in the spatial distribution of said parameter, with cold spots being on the left tail and hot spots on the right tail of the distribution. There are two main approaches to the analysis of spatial autocorrelation. Measures of global spatial autocorrelation such as Moran's I (Moran, 1950) and Geary's C (Geary, 1954) estimate the overall degree of spatial interdependence between regions. Local spatial autocorrelation, on the other hand, allows for local heterogeneity even in the presence of global autocorrelation.

To investigate the presence of regions with an elevated concentration of high-hazard/exposure/risk electoral divisions, we compute the Getis-Ord $G_i^*(d)$ measure of local spatial autocorrelation (Getis and Ord, 1992). This is given by,

$$G_i^* = \frac{\sum_{j=1}^{J} w_{ij}(d)x_j}{\sum_{j=1}^{J} x_j},\ \text{for } j \neq i \tag{12}$$

where w_{ij} is a weight matrix, d is the distance from a reference point, and x is a variable of interest. Hence, for each spatial observation i, the Getis-Ord statistic is the ratio between the local sum of variable x for all areas j within a radius d from the reference point (e.g. the centroid of electoral division i) and the overall sum of x in the reference macroregion (e.g. a country). In our analysis, we adopt a symmetric 0/1 binary weight matrix, meaning that electoral divisions are included in the local sum if their centroids are within the radius d from i's centroid and they are excluded otherwise. An extension of the basic formulation which allows for non-binary weights is presented in Ord and Getis (1995).

4 Results

This section presents the flood hazard, exposure and risk hot spots, based on the Getis-Ord $G_i^*(d)$ local spatial autocorrelation discussed in Section 3.5. The local spatial autocorrelation analysis identifies both hot and cold spots, but since the scope of this paper is to assess the more vulnerable areas, in the maps reported below we only display hot spots. Also, electoral divisions that have a population at risk of flooding greater than their total population, as discussed in Section 3.2, are removed from the analysis of flood exposure

and flood risk.[19] We use $d = 10$ km as a distance parameter (for comparison, the average area of electoral divisions is 20.61 squared kilometers).[20]

In addition to the hot spots maps, in Appendix B we also present tables listing the twenty most affected electoral divisions according to their level of flood hazard, exposure and risk. In all tables, the fourth column reports the values of flood hazard, exposure and risk based on Equations 1, 4 and 10, respectively; whereas the fifth column reports the corresponding indices derived in Equations 2, 5 and 11.

4.1 Flood hazard

We want to assess the contribution of each additional piece of information, to provide decision makers with a multidimensional representation of flood vulnerability. We set off by considering flood hazard, which provides insights on the physical area affected by flooding.

Figure 5 displays the classification of Irish electoral divisions according to their flood hazard index (panel (a)) and the corresponding flood hazard hot spots (panel (b)). The distribution of flood hazard maps mirrors the flood extents displyed in Figure 1, with the higher hazard areas and main hot spots located on the course and estuary of the Shannon river, on the high course of the Barrow river, on the north-eastern coast in the cities of Dublin and Dundalk, on the western coast on the estuary of the Feale river and in the city of Galway, and in the Lough Conn area. Table B2 in Appendix B, reports the top twenty electoral divisions based on their level of flood hazard. It confirms that the most affected areas are the cities of Dublin, Dundalk and Limerick.

4.2 Flood exposure

Incorporating population exposure considerably changes the distribution of most vulnerable areas. As it can be seen from Figure 6, while Dublin, Dundalk, Ennis, Galway and Limerick remain amongst the most affected areas, there are no longer hot spots (Figure 6b) along the course of the Shannon river, on the estuary of the Feale river and in the Lough Conn area. This is likely due to electoral divisions in those areas being scarcely inhabited and with the majority of their population distributed away from the parts at risk of being inundated. Hence, despite presenting considerable flood hazard levels, they do not represent a major concern in terms of exposure.

4.3 Flood risk

Figure 7 displays the flood risk map (panel (a)) and hot spots (panel (b)), derived using the percentage of an electoral division's households at risk of poverty (AROP) as the measure of social vulnerability. The results resembles the distribution of flood exposure displayed in Figure 6, albeit with some differences.

As it can be seen from Figure 7a, there are considerably more electoral divisions in the lower risk classes. Conversely, the higher risk classes contain roughly half of the entries, as shown also in Table B5. This is not surprising, since, for example, shoreline areas are inhabited predominantly by more affluent households who can afford to pay a price premium to enjoy the scenic view (Breil et al., 2021). This is, for instance, the case of Pembroke East B and C in the city of Dublin, which rank amongst the most affected EDs for flood

[19] Since no issue emerges with flood hazard, we have decided to include them in that part of the analysis.

[20] Other distance parameters have been tested. Smaller values smaller led to several hot spots being given by individual electoral divisions. Bigger values primarily enlarged the hot spots identified with $d = 10$. For these reasons, we have chosen 10 kilometers as our preferred distance parameter.

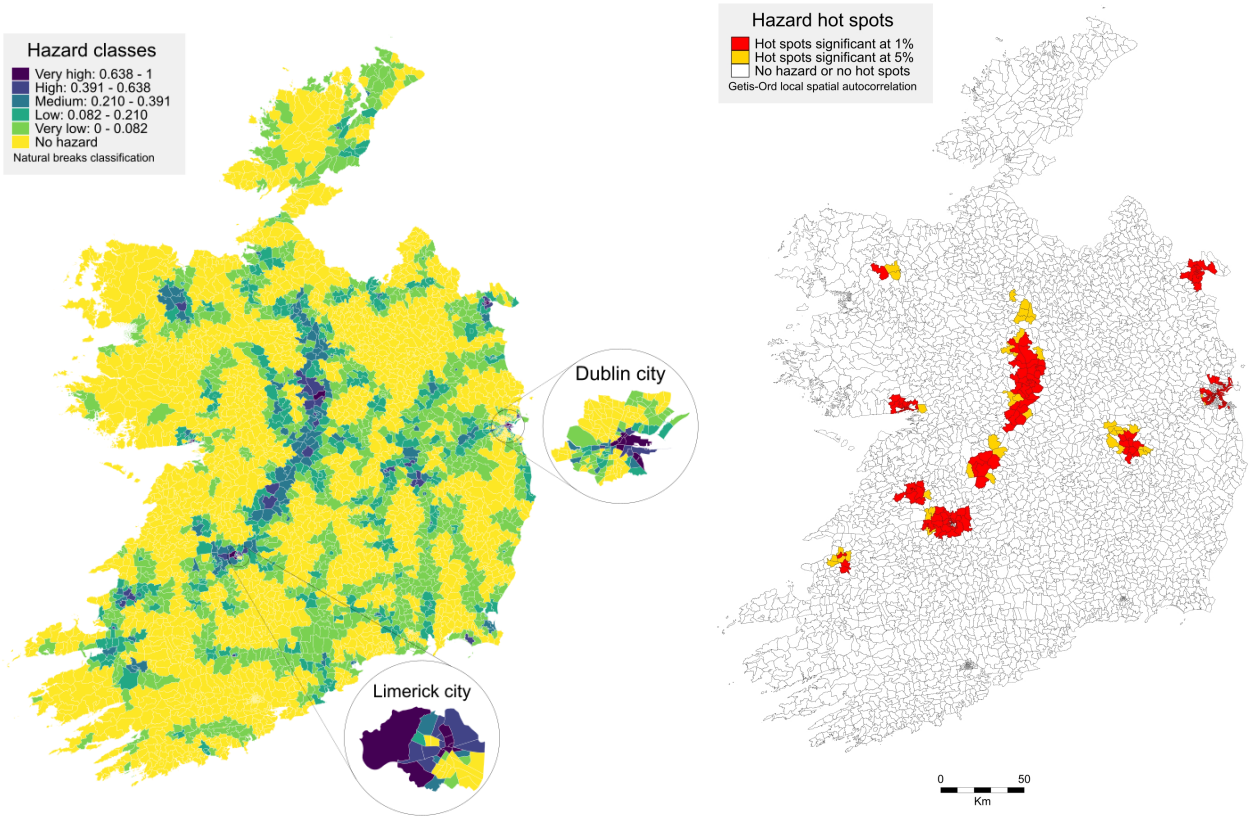

(a) Flood hazard index

(b) Flood hazard hot spots

Figure 5: Flood hazard maps

Notes. This figure displays the flood hazard index (a) and hot spots (b). The flood hazard index, derived according to Equation 2, is divided five classes using a natural break classification. The actual natural breaks are as follows: very low hazard = [2.2e-07; 0.081431]; low hazard = [0.082195; 0.209583]; medium hazard = [0.211146; 0.391361]; high hazard = [0.398398; 0.63778]; very high hazard = [0.675216; 1]. Electoral divisions not affected by flooding are assigned a value of 0 and are included into a 'No hazard' class. Hot spots are derived according to the Getis-Ord $G_i^*(d)$ local spatial autocorrelation.

hazard and exposure, but, in light of their wealthy population, are classified only at medium-low risk. These difference are confirmed in Table B6, where the set of most vulnerable EDs is considerably different from those reported in Tables B2 and B4, both in terms of composition (there are eight new entries) and ranking.

Looking at Figure 7b, we can see that the composition of flood risk hot spots is only marginally different from exposure ones, with some becoming smaller or less significant in line with the pattern evidenced above. More importantly, there are no new hot spots appearing. This allows us to already make a first consideration. Namely, that flood exposure, by itself, seems to offer a good approximation of flood vulnerability and of the areas of priority.

4.3.1 Alternative measures of socio-economic vulnerability

The maps displayed in Figure 7 use the percentage of households in an electoral division at risk of poverty as the social vulnerability dimension to compute social weights (Equation 9) and to derive flood risk (Equation 10). However, as said in Section 3.4, financial hardship is far from being the only channel through which social vulnerability can exacerbate climate impacts. So, Figure 8 reports the results obtained using alternative measures of social vulnerability. Specifically, Figures 8a and 8b adopt the percentage of households in an

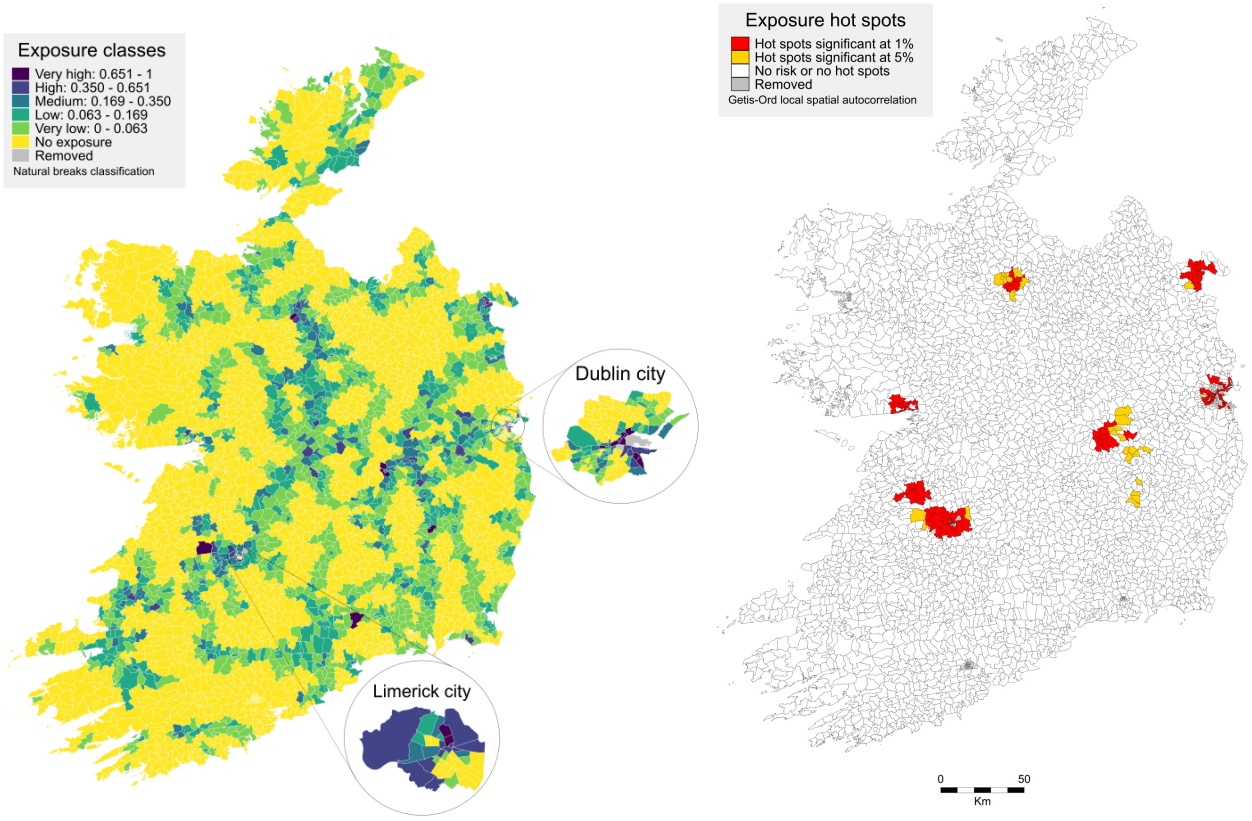

(a) Flood exposure index

(b) Flood exposure hot spots

Figure 6: Flood exposure maps

Notes. This figure displays the flood exposure index (a) and hot spots (b). The flood exposure index, derived according to Equation 5, is divided five classes using a natural break classification. The actual natural breaks are as follows: very low exposure = [3.6e-06; 0.063364]; low exposure = [0.063692; 0.168826]; medium exposure = [0.170852; 0.349739]; high exposure = [0.367115; 0.650818]; very high exposure = [0.674369; 1]. Electoral divisions not affected by flooding are assigned a value of 0 and are included into a 'No exposure' class. Hot spots are derived according to the Getis-Ord $G_i^*(d)$ local spatial autocorrelation. Electoral divisions with percentage of population affected by flooding > 1 and percentage of area affected by flooding < 0.9 have been removed.

electoral division that derive the majority of their income from old-age pension, while Figures 8c and 8d the percentage of households in an electoral division that derive the majority of their income from old-age pension and are also at risk of poverty.

A comparison of panels (a)-(b) with Figure 7 shows many similarities, The distribution of flood risk closely resembles that observed with AROP, but also several differences. In particular, the hot spot in the city of Dublin becomes smaller, now located exclusively in the northern coastal area. Conversely, the hot spot in the upper course of the Shannon river gets bigger. In addition, there is a reappearance of a hot spot on the estuary of the Feale river on the western coast.

In panels (c)-(d) there are additional changes, especially for what concerns the hot spots. These appear generally smaller that those seen for the AROP and OPA separately. The biggest difference is the emergence of a hot spot in the Wexford area on the south-eastern coast (significant at the 10% level). Finally, Table B10 reports the twenty electoral divisions at highest risk. For the most part they are a combination of those appearing in Tables B6 and B8. These results confirm the importance of a careful selection of the vulnerability dimensions to be considered when planning adaptation interventions.

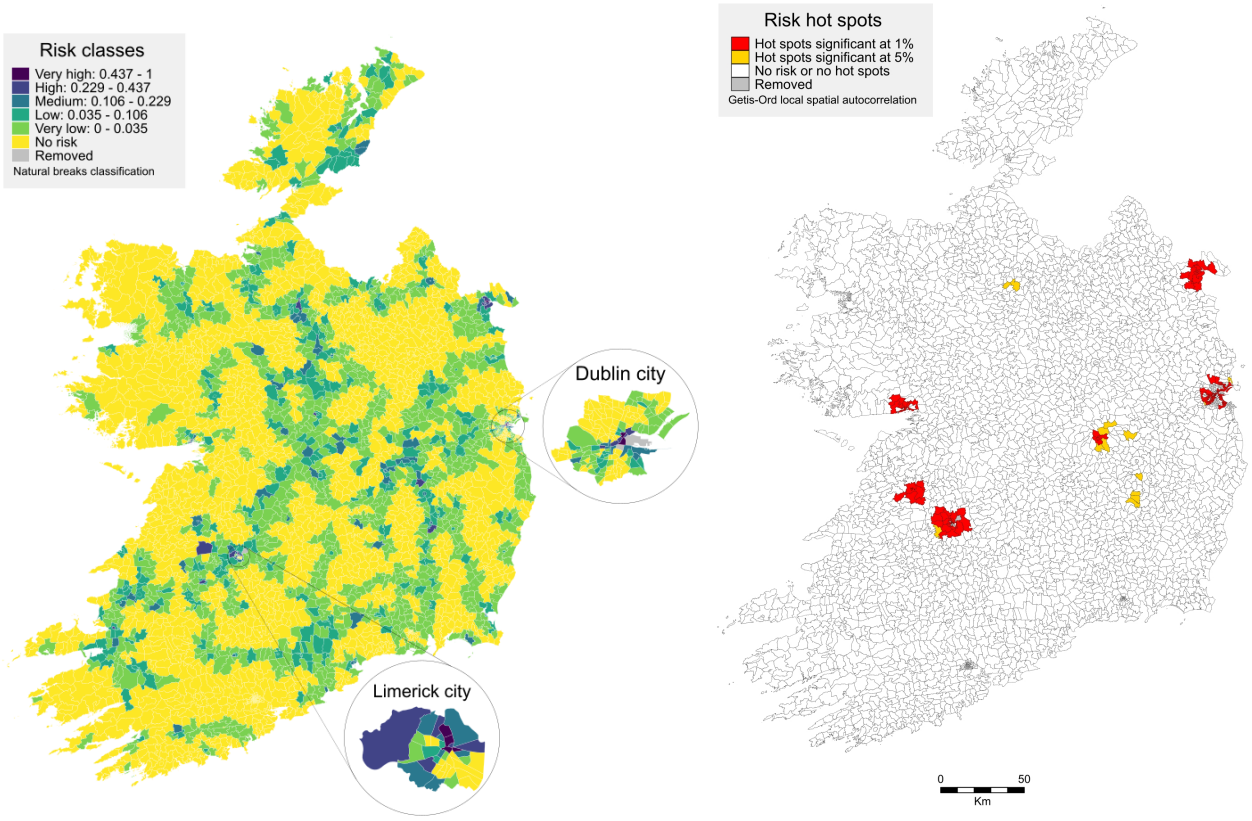

(a) Flood risk index

(b) Flood risk hot spots

Figure 7: Flood risk maps — AROP

Notes. This figure displays the flood risk index (a) and hot spots (b). The social vulnerability measure used to compute social weights is the percentage of electoral division's households at risk of poverty. The flood risk index, derived according to Equation 11, is divided five classes using a natural break classification. The actual natural breaks are as follows: very low risk = [1.1e-06; 0.035474]; low risk = [0.035741; 0.10508]; medium risk = [0.106666; 0.228676]; high risk = [0.234423 - 0.436813]; very high risk = [0.51337; 1]. Electoral divisions not affected by flooding are assigned a value of 0 and are included into a 'No risk' class. Hot spots are derived according to the Getis-Ord $G_i^*(d)$ local spatial autocorrelation. Electoral divisions with percentage of population affected by flooding > 1 and percentage of area affected by flooding < 0.9 have been removed.

4.3.2 The effect of redistribution preferences

As discussed in Section 3.4, the social weights used to derive flood risk depend of the selection of the redistribution parameter e. The results displayed above are obtained for a value $e = 1$, but there is no guarantee that this actually reflects the true redistribution preferences. Hence, in order to investigate how the choice of e affects flood risk and the distribution of hot spots, we repeat the analysis using different values of the parameter. More specifically, we first set $e = 1.5$, which corresponds to the upper bound of the values typically adopted in the literature (Cline, 1992; Fankhauser et al., 1997). Then, we test two further values above this level, namely $e = 3$ and $e = 5$, to assess how the picture would change if the social planner put an even greater importance to inequality and social vulnerability. In light of the concerns about climate impacts having a greater toll on more vulnerable constituencies and of the principles of just resilience, we decide not to examine instances with $e < 1$. However, notice that flood exposure corresponds to $e = 0$ — i.e. a situation of inequality neutrality, in which all that matters is that the highest number of individuals are protected but there is no extra benefit to reducing inequality.

Figure 9 displays the flood risk hot spots for these values of e. When AROP is used as a measure of socio-economic vulnerability (panel (a)), as the value of e increases the number of hot spots decreases and their extension shrinks. This is due to the fact that, as more importance is put to inequality, the weight assigned to the most vulnerable electoral divisions, and consequently their value of flood risk, rise exponentially in comparison to the remaining ones. The result is a smaller set of high-risk electoral divisions and a bigger set of medium- and low-risk ones. It is only when using larger values of e that more considerable changes emerge. With $e = 3$ (middle figure of panel (a)) the Galway hot spot disappears and the Dublin and Ennis ones are reduced to a handful of electoral divisions only significant at the 10% level. With $e = 5$ (right figure of panel (a)), the only remaining hot spot is in the Limerick area, on the estuary of the Shannon river.

Also in panel (b) when OAP is used as socio-economic vulnerability dimension, increasing e well beyond the values typically adopted in the literature does not significantly alter the picture. The distribution and composition of hot spots remains comparable to those observed in Figure 8b with $e = 1$, again with a general trend of decrease in their number and extension. Some differences do emerge however. Most notably represented by the hot spot at the mouth of the Feale river, which becomes wider as e increases. And by the emergence of two new hot spots along the cource of the Shannon River and in the centre-north.

When both economic and physical vulnerability are considered simultaneously (panel (c)), we see a more pronounced effect of the redistribution parameter. Already an increase to $e = 1.5$ leads to a change in composition of the hot spots, with the one on the south-eastern coast, in the Wexford area, becoming wider and more significant; those in Galway and in the upper course of the Shannon river disappearing; and an new one emerging on the western coast. As we further increase e beyond values typically used in the literature, another hot spot in the upper course of the Shannon river appears, and those in the south-western and western coast becomes more extended significant at the 1% level, while most of the others fade away.

From this, we can draw additional considerations with important policy implications. Moreover, with values of inequality aversion commonly adopted in the literature ($e \leqslant 1.5$), the flood risk hot spots are very similar to flood exposure ones. Only when values considerably larger are adopted does the picture change. In most cases the change corresponds to a decrease in the the number and extension of hot spots. Does this mean that considering social vulnerability profiles is unnecessary? The answer is no. In facts, while flood exposure provides a good approximation of the areas of priority of intervention, enriching the analysis with information on social vulnerability allows policymakers to narrow the focus on those areas of *highest* priority, based on the specific views of justice and redistribution. In addition, there are differences in terms of the effect of the redistribution parameter across socio-economic vulnerability measures, which further highlights the importance of a careful evaluation of the desired effects in terms of reducing flood risk and inequality. This should reduce the risk of interventions being mis-targeted and ensure a more efficient allocation of resources.

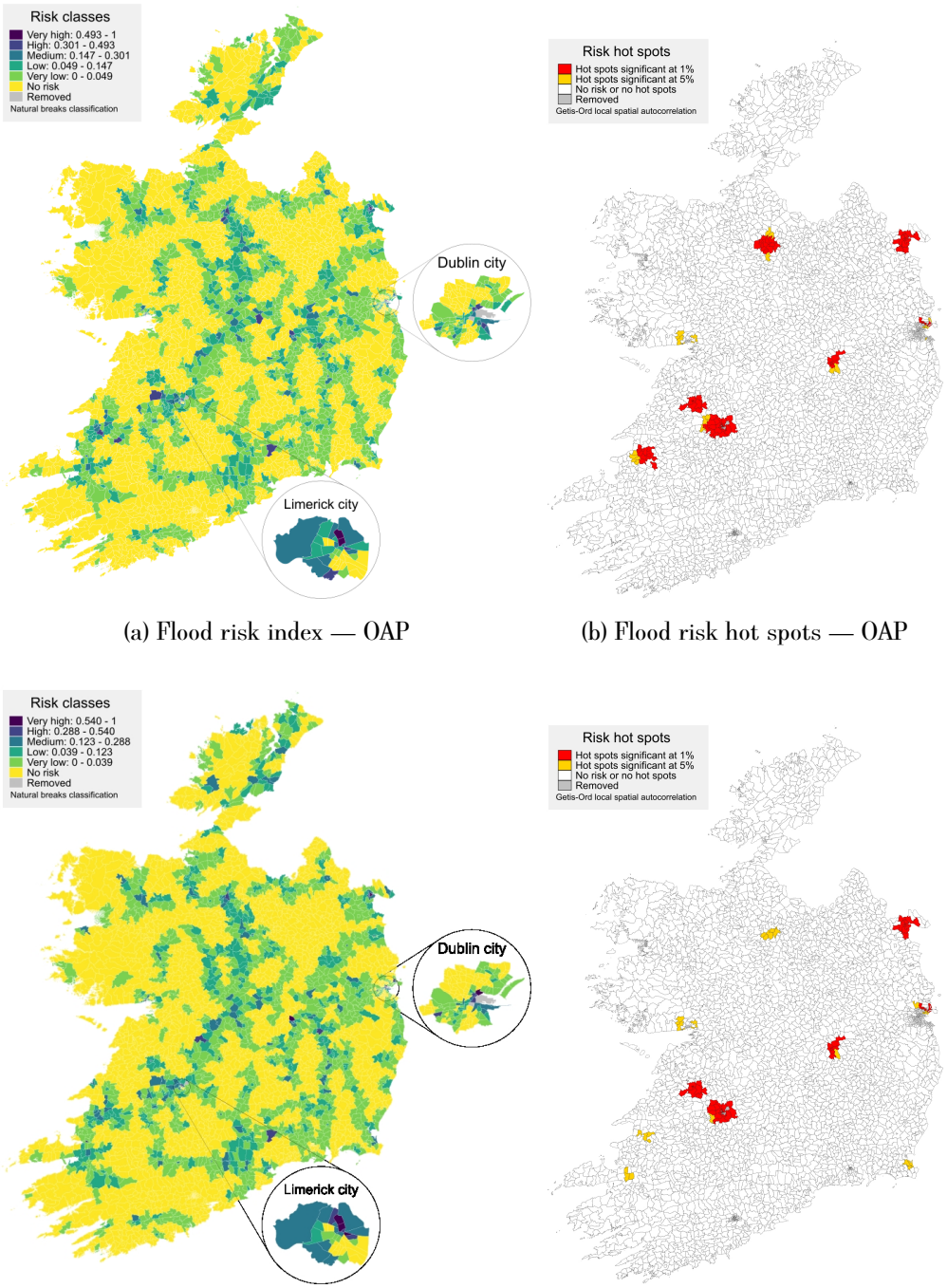

(a) Flood risk index — OAP

(b) Flood risk hot spots — OAP

(c) Flood risk index — OAP + AROP

(d) Flood risk hot spots — OAP + AROP

Figure 8: Flood risk maps — Alternative dimensions of socio-economic vulnerability

Notes. This figure displays the flood risk indexes and hot spots for alternative measures of social vulnerability. In panels (a) and (b) the socio-economic vulnerability measure is the percentage of electoral division's households that derive the majority of their income from old-age pension. In panels (c) and (d) the socio-economic vulnerability measure is the percentage of electoral division's households that derive the majority of their income from old-age pension and are also at risk of poverty. The flood risk indexes, derived according to Equation 11, are divided five classes using a natural break classification. The actual natural breaks for panel (a) are: very low risk = [2.1e-06; 0.048513]; low risk = [0.049013; 0.146723]; medium risk = [0.14863; 0.300699]; high risk = [0.329929; 0.493007]; very high risk = [0.647374; 1]. Whereas for panel (c) they are: very low risk = [0; 0.039556]; low risk = [0.039705; 0.123727]; medium risk = [0.125733; 0.288267]; high risk = [0.314442; 0.539967]; very high risk = [0.617191; 1]. Electoral divisions not affected by flooding are assigned a value of 0 and are included into a 'No risk' class. Hot spots are derived according to the Getis-Ord $G_i^*(d)$ local spatial autocorrelation. Electoral divisions with percentage of population affected by flooding > 1 and percentage of area affected by flooding < 0.9 have been removed.

(a) AROP

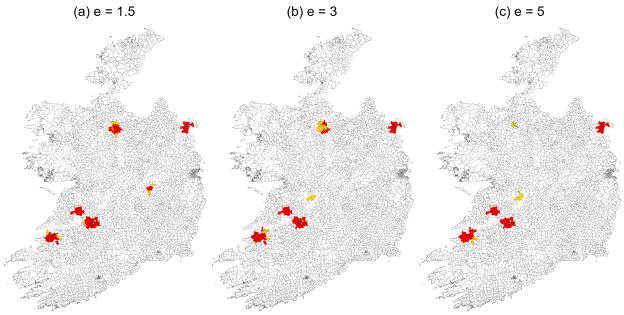

(b) OAP

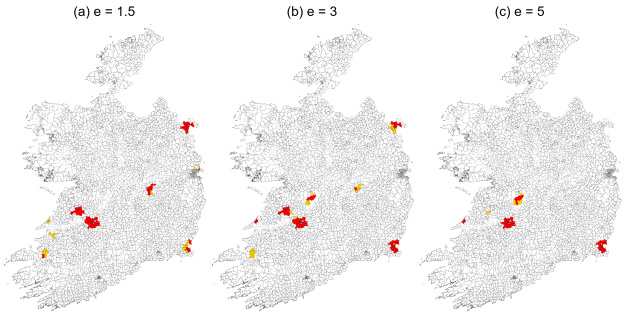

(c) OAP + Arop

Figure 9: Hot spots with different redistribution parameters

Notes. This figure displays the flood hazard index (a) and hot spots (b). The flood hazard index, derived according to Equation 2, is divided five classes using a natural break classification. The actual natural breaks are as follows: very low hazard = [2.2e-07; 0.081431]; low hazard = [0.082195; 0.209583]; medium hazard = [0.211146; 0.391361]; high hazard = [0.398398; 0.63778]; very high hazard = [0.675216; 1]. Electoral divisions not affected by flooding are assigned a value of 0 and are included into a 'No hazard' class. Hot spots are derived according to the Getis-Ord $G_i^*(d)$ local spatial autocorrelation.

5 Conclusion

This paper evaluates the importance of incorporating socioeconomic vulnerability in the quantification of climate impacts. We present the application of a small area estimation technique using an Irish case study, providing a more granular quantification of climate risk relative to that common in the literature. We demonstrate that while population exposure offers insight into flood risk patterns, the introduction of socioeconomic vulnerability allows a more precise identification of areas of priority. Such prioritisation varies with societal preferences towards justice and equity. This result highlights the importance of both spatial profiles of climate impacts and socioeconomic vulnerabilities in effectively targeting climate adaptation interventions.

This paper presents several novelties and relevant contributions. It is the first large-scale evaluation of climate risk with a high degree of spatial detail. This is made possible by the use of a small area estimation technique that allows the production of spatially representative socioeconomic profiles which would not be otherwise available. Incorporating said profiles with climate vulnerability, we are able to provide a more detailed assessment of climate risk than in previous studies. The outcomes thus generated offer reliable evidence to inform policy decision-making. In addition, the application of small area estimation techniques to climate risk assessment represents a novelty in the small area estimation and spatial microsimulation literature.

The results of this paper present important policy implications. The difference between flood hazard and flood exposure patterns demonstrate the need to include considerations of affected population in climate adaptation interventions. Flood exposure offers a first overview of locations that may require adaptation interventions when no extra social utility is derived from reducing inequality. If policymakers want to simultaneously address socioeconomic vulnerabilities, the analysis highlights the importance to precisely establish the preferences toward equity. In fact, these are key in determining the locations of highest priority.

There are many conceivable extensions to the analysis of this paper. First, it should be emphasised that this analysis presents a specific case study example using particular OPW CFRAMS scenarios. Each scenario features a different set of flood risks. For instance, the fluvial (riverflow) scenarios do not consider regions affected by other types of flooding, such as Cork City or some flooding in Galway. These flood risks are captured by other flood scenarios. The purpose of this paper is to demonstrate the application of this methodology using a suitable dataset, and therefore the flood scenarios presented is determined by the datasets chosen to demonstrate the model that is used. As such, this paper does not contain a full account of flood vulnerability in Ireland. Future work may expand on this to consider a more comprehensive suite of flooding events in Ireland.

Second, it has been argued that social vulnerability should be considered in a holistic perspective, incorporating multiple dimensions. The incorporation of multidimensional poverty indices in climate impact analysis represents a natural extension of this paper (indeed, the results presented in Sections 4.3.1 and 4.3.2 do support the view that there is merit in evaluating multiple dimensions of vulnerability). Third, the methodology presented in the paper may be applied in the analysis of further climate shocks. For instance, rising temperatures are increasing the levels of heat stress in many part of the world, with adverse effects more severe among vulnerable individuals. Extending the investigation to other climate impacts would provide important insights for policy decision-making. Finally, it is worth noting that the analysis presented in this paper offers a static picture of climate and socioeconomic vulnerability. It does not consider the evolution

of these factors over time and any potential sorting effects, where wealthy households avoid settlement in locations subject to climate impacts. The link between population sorting and other climate shocks remains an important topic that should be further explored. The methods of analysis presented in this paper provide an appropriate platform.

References

Anthoff, D., Hepburn, C. and Tol, R. S. J. (2009). Equity weighting and the marginal damage costs of climate change. *Ecological Economics* 68: 863–849, doi:10.1016/j.ecolecon.2008.06.017.

Azar, C. (1999). Weight Factors in Cost-Benefit Analysis of Climate Change. *Environmental and Resource Economics* 13: 249–268, doi:10.1023/A:1008229225527.

Azar, C. and Sterner, T. (1996). Discounting and distributional considerations in the context of global warming. *Ecological Economics* 19: 169–184, doi:10.1016/0921-8009(96)00065-1.

Baer, P. (2009). Equity in climate-economy scenarios: the importance of subnational income distribution. *Environmental Research Letters* 4: 015007, doi:10.1088/1748-9326/4/1/015007.

Barnett, B. J., Barrett, C. B. and Skees, J. R. (2008). Poverty traps and index-based risk transfer products. *World Development* 36: 1766–1785, doi:10.1016/j.worlddev.2007.10.016.

Breil, M., Zandersen, M., Pishmisheva, P., Branth Pedersen, A., Romanovska, L., Coninx, I., Rogger, M. and Johnson, K. (2021). 'Leaving No One Behind' in Climate Resilience Policy and Practice in Europe. European Topic Centre on Climate Change impacts, Vulnerability and Adaptation (ETC/CCA) Technical Paper 2021/2, doi:10.1080/08941921003652940.

Broome, J. (1991). *Weighing Goods: Equality, Uncertainty and Time*. Blackwell, Oxford, United Kingdom.

Centre for Research on the Epidemiology of Disasters and United Nations Office for Disaster Risk Reduction (2020). The human cost of disasters: An overview of the last 20 years (2000-2019). Available at: https://www.preventionweb.net/files/74124_humancostofdisasters20002019reportu.pdf?_gl=1*12ztamc*_ga*MzA4MTU5ODk0LjE2OTY0MTYxNTY.*_ga_D8G5WXP6YM*MTY5NzYyMDg5MS4yLjEuMTY5NzYyMDkwNS4wLjAuMA.. (accessed October 18, 2023).

Chan, N. W. and Sayre, S. S. (Forthcoming). Spatial microsimulation of carbon tax incidence: An application to Washington State. *Journal of the Association of Environmental and Resource Economists* doi:10.1086/727476.

Citeau, J.-M. (2003). A New Control Concept in the Oise Catchment Area, Definition and Assessment of Flood Compatible Agricultural Activities. FIG working week, Paris, France, 2003.

Cline, W. R. (1992). The Economics of Global Warming.

Cowell, F. A. and Gardiner, K. (1999). Welfare Weights. OFT Economic Research Paper. Office of Fair Trading, London.

Cullinan, J. (2011). A Spatial Microsimulation Approach to Estimating the Total Number and Economic Value of Site Visits in Travel Cost Modelling. *Environmental and Resource Economics* 50: 27–47, doi:10.1007/s10640-011-9458-x.

Cummins, J. and Mahul, O. (2009). *Catastrophe Risk Financing in Developing Countries: Principles for Public Intervention*. The World Bank, Washington, D.C.

DEFRA (2006). Flood Risk to People Phase 2, FD2321/TR2 Guidance Document. Department for Environment, Food and Rural Affairs, London, UK, March 2006.

Desmond, M., O'Brien, P. and McGovern, F. (2017). A Summary of the State of Knowledge on Climate Change Impacts for Ireland. EPA Research Programme 2014-2020, Report No. 223.

Elbers, C., Lanjouw, J. O. and Lanjouw, P. (2003). Micro-Level Estimation of Poverty and Inequality. *Econometrica* 71: 355–364, doi:10.1111/1468-0262.00399.

Escuder-Bueno, I., Castillo-Rodríguez, J. T., Zechner, S., Jöbstl, C., Perales-Momparler, S. and Petaccia, G. (2012). A quantitative flood risk analysis methodology for urban areas with integration of social research data. *Natural hazards and earth system sciences* 12: 2843–2863.

European Commission (2021). Communication from the Commission to the European parliament, the Council, the European economic and social committee and the Committee of the regions: Forging a climate-resilient Europe - the new EU Strategy on Adaptation to Climate Change. COM(2021) 82 final. https://eur-lex.europa.eu/legal-content/EN/TXT/?uri=COM%3A2021%3A82%3AFIN.

European Environment Agency (2023). Economic losses from climate-related extremes in Europe (8th EAP). Available at: https://www.eea.europa.eu/ims/economic-losses-from-climate-related (accessed October 4, 2023).

European Parliament and Council of the European Union (2003). Regulation (EC) No 1177/2003 of the European Parliament and of the Council of 16 June 2003 concerning Community statistics on income and living conditions (EU-SILC) (Text with EEA relevance) OJ L 165, 3.7.2003, p. 1-9. https://eur-lex.europa.eu/legal-content/EN/TXT/PDF/?uri=CELEX:32003R1177&from=EN.

European Parliament and Council of the European Union (2007). Directive 2007/60/EC of the European Parliament and of the Council of 23 October 2007 on the assessment and management of flood risks (Text with EEA relevance) OJ L 288, 6.11.2007, p. 27-34. https://eur-lex.europa.eu/legal-content/EN/TXT/?uri=CELEX:32007L0060.

Fankhauser, S., Tol, R. S. J. and Pearce, D. W. (1997). The Aggregation of Climate Change Damages: A Welfare Theoretic Approach. *Environmental and Resource Economics* 10: 249–266, doi:10.1023/A:1026420425961.

Farrell, N. (2023). Small Area Estimation by Conditional Monte Carlo: Robust, Micro-level Inference. ESRI Working Paper.

Farrell, N., Morrissey, K. and O'Donoghue, C. (2013). Creating a Spatial Microsimulation Model of the Irish Local Economy. In Tanton, R. and Edwards, K. L. (eds), *Spatial Microsimulation: A Reference Guide for Users*. Dordrecht: Springer Netherlands, 105–125, doi:10.1007/978-94-007-4623-7.

Field, C. B., Barros, V., Stocker, T. F. and Dahe, Q. (2012). *Managing the risks of extreme events and disasters to advance climate change adaptation: special report of the intergovernmental panel on climate change*. Cambridge University Press.

Geary, R. C. (1954). The Contiguity Ratio and Statistical Mapping. *The Incorporated Statistician* 5: 115–146, doi:10.2307/2986645.

Getis, A. and Ord, J. K. (1992). The analysis of spatial association by use of distance statistics. *Geographical Analysis* 24: 189–206, doi:10.1111/j.1538-4632.1992.tb00261.x.

Giupponi, C., Mojtahed, V., Gain, A. K., Biscaro, C. and Balbi, S. (2015). Integrated Risk Assessment of Water-Related Disasters. In Shroder, J. F., Paron, P. and Baldassarre, G. D. (eds), *Hydro-Meteorological Hazards, Risks, and Disasters*. Elsevier, 163–200, doi:10.1016/B978-0-12-394846-5.00006-0.

Global Commission on Adaptation (2019). Adapt Now: A Global Call for Leaders on Climate Resilience. Global Center on Adaptation, and World Resources Institute.

Hallegatte, S., Bangalore, M., Bonzanigo, L., Fay, M., Kane, T., Narloch, U., Rozenberg, J., Treguer, D. and Vogt-Schilb, A. (2016). Shock Waves : Managing the Impacts of Climate Change on Poverty. Climate Change and Development;. Washington, DC: World Bank.

Hallegatte, S. and Rozenberg, J. (2017). Climate change through a poverty lens. *Nature Climate Change* 7: 250–256, doi:10.1038/nclimate3253.

Hayek, F. A. (1960). *The Constitution of Liberty*. University of Chicago Press, Chicago, IL.

Hudson, P. (2018). A comparison of definitions of affordability for flood risk adaption measures: a case study of current and future risk-based flood insurance premiums in europe. *Mitigation and Adaptation Strategies for Global Change* 23: 1019–1038, doi:doi.org/10.1007/s11027-017-9769-5.

Hudson, P., Botzen, W. W., Feyen, L. and Aerts, J. C. (2016). Incentivising flood risk adaptation through risk based insurance premiums: Trade-offs between affordability and risk reduction. *Ecological Economics* 125: 1–13, doi:10.1016/j.ecolecon.2016.01.015.

Hynes, S., Morrissey, K., O'Donoghue, C. and Clarke, G. (2009). A spatial micro-simulation analysis of methane emissions from Irish agriculture. *Ecological Complexity* 6: 135–146, doi:10.1016/j.ecocom.2008.10.014.

IPCC (2022). Climate Change 2022: Impacts, Adaptation and Vulnerability. Contribution of Working Group II to the Sixth Assessment Report of the Intergovernmental Panel on Climate Change [H.-O. Pörtner, D.C. Roberts, M. Tignor, E.S. Poloczanska, K. Mintenbeck, A. Alegría, M. Craig, S. Langsdorf, S. Löschke, V. Möller, A. Okem, B. Rama (eds.)]. Cambridge University Press. Cambridge University Press, Cambridge, UK and New York, NY, USA, 3056 pp., doi:10.1017/9781009325844.

Kazama, S., Sato, A. and Kawagoe, S. (2009). Evaluating the cost of flood damage based on changes in extreme rainfall in japan. *Sustainability Science* 4: 61–69, doi:10.1007/s11625-008-0064-y.

Kilgarriff, P., McDermott, T. K. J., Vega, A., Morrissey, K. and O'Donoghue, C. (2019). The impact of flooding disruption on the spatial distribution of commuter's income. *Journal of Environmental Economics and Policy* 8: 48–64, doi:10.1080/21606544.2018.1502098.

Lindley, S., O'Neill, J., Kandeh, J., Lawson, N., Christian, R. and O'Neill, M. (2011). Climate change, justice and vulnerability. Joseph Rowntree Foundation (JRF), York (UK). Available at: https://www.jrf.org.uk/report/climate-change-justice-and-vulnerability.

Madsen, H., Lawrence, D., Lang, M., Martinkova, M. and Kjeldsen, T. R. (2013). A review of applied methods in Europe for flood-frequency analysis in a changing environment. NERC/Centre for Ecology & Hydrology, 180pp. (ESSEM COST Action ES0901).

Molina, I. and Rao, J. N. K. (2010). Small area estimation of poverty indicators. *The Canadian Journal of Statistics* 38: 369–385, doi:10.1002/cjs.10051.

Moran, P. A. P. (1950). Notes on Continuous Stochastic Phenomena. *Biometrika* 37: 17–23, doi:10.2307/2332142.

Nolan, P. and Flanagan, J. (2020). High-resolution Climate Projections for Ireland – A Multi-model Ensemble Approach. EPA Research Programme 2014-2020, Report No. 339.

Nozick, R. (1974). *Anarchy, State, and Utopia*. New York: Basic Books.

O'Donoghue, C., Farell, N., Morrissey, K., Lennon, J., Ballas, D., Clarke, G. and Hynes, S. (2013). The SMILE Model: Construction and Calibration. In O'Donoghue, C., Ballas, D., Clarke, G., Hynes, S. and Morrissey, K. (eds), *Spatial Microsimulation for Rural Policy Analysis. Advances in Spatial Science.*. Springer, Berlin, Heidelberg, 55–86, doi:10.1007/978-3-642-30026-4_4.

Olbert, A. I., Hartnett, M., Comer, J. and Nash, S. (2022). Mechanisms of flooding in Cork City. National Hydrology Conference.

Ord, J. K. and Getis, A. (1995). Local Spatial Autocorrelation Statistics: Distributional Issues and an Application. *Geographical Analysis* 27: 286–306, doi:10.1111/j.1538-4632.1995.tb00912.x.

Park, J., Bangalore, M., Hallegatte, S. and Sandhoefner, E. (2018). Households and heat stress: estimating the distributional consequences of climate change. *Environment and Development Economics* 23: 349–368, doi:10.1017/S1355770X1800013X.

Parry, M. L., Canziani, O., Palutikof, J. P., van der Linden, P. and Hanson, C. (2007). Climate Change 2007: Impacts, Adaptation and Vulnerability. Contribution of Working Group II to the Fourth Assessment Report of the Intergovernmental Panel on Climate Change. Cambridge: Cambridge University Press.

Pearce, D. W. (2003). The social cost of carbon and its policy implications. *Oxford Review of Economic Policy* 19: 362–384, doi:http://www.jstor.org/stable/23606756.

Pearce, D. W. and Ulph, D. (1994). Estimating a social discount rate for the United Kingdom, mimeo. Centre for Social and Economic Research on the Global Environment. University College London and University of East Anglia.

Programme, U. N. E. (2021). Adaptation Gap Report 2020. Nairobi.

Rao, N. D., van Ruijven, B. J., Riahi, K. and Bosetti, V. (2017). Improving poverty and inequality modelling in climate research. *Nature Climate Change* 7: 857–862, doi:10.1038/s41558-017-0004-x.

Rawls, J. (1971). *A Theory of Justice*. Harvard University Press.

Ronco, P., Gallina, V., Torresan, S., Zabeo, A., Semenzin, E., Critto, A. and Marcomini, A. (2014). The KULTURisk Regional Risk Assessment methodology for water-related natural hazards - Part 1: Physical-environmental assessment. *Hydrology and Earth System Sciences* 18: 5399–5414, doi:10.5194/hess-18-5399-2014.

Ryan, P. C., Hawchar, L., Naughton, O. and Stewart, M. G. (2021). CIViC: Critical Infrastructure Vulnerability to Climate Change. EPA Research Programme 2021-2030, Report No. 369.

Salvati, N., Tzavidis, N., Pratesi, M. and Chambers, R. (2010). Small area estimation via M-quantile geographically weighted regression. *TEST* 21: 1–28, doi:10.1007/s11749-010-0231-1.

Sánchez, M. V. (2018). Climate Impact Assessments With a Lens on Inequality. *The Journal of Environment & Development* 27: 267–298, doi:10.1177/1070496518774098.

Sanchez-Guevara, C., Núñez Peiró, M., Taylor, J., Mavrogianni, A. and Neila González, J. (2019). Assessing population vulnerability towards summer energy poverty: Case studies of Madrid and London. *Energy & Buildings* 190: 132–143, doi:10.1016/j.enbuild.2019.02.024.

Schelling, T. C. (1992). Some Economics of Global Warming. *The American Economic Review* 82: 1–14.

Sovacool, B. K., Linnèr, B.-O. and Goodsite, M. E. (2015). The political economy of climate adaptation. *Nature Climate Change* 5: 616–618, doi:10.1038/nclimate2665.

Sperotto, A., Torresan, S., Gallina, V., Coppola, E., Critto, A. and Marcomini, A. (2016). A multi-disciplinary approach to evaluate pluvial floods risk under changing climate: The case study of the municipality of Venice (Italy). *Science of the Total Environment* 562: 1031–1043, doi:10.1016/j.scitotenv.2016.03.150.

Szewrański, S., Świąder, M., Kazak, J. K., Tokarczyk-Dorociak, K. and van Hoof, J. (2018). Socio-Environmental Vulnerability Mapping for Environmental and Flood Resilience Assessment: The Case of Ageing and Poverty in the City of Wrocław, Poland. *Integrated Environmental Assessment and Management* 14: 592–597, doi:10.1002/ieam.4077.

Tanner, T., Surminski, S., Wilkinson, E., Reid, R., Rentschler, J. and Rajput, S. (2015). The triple dividend of resilience. realising development goals through the multiple benefits of disaster risk management. Overseas Development Institute, Global Facility for Disaster Risk Reduction, and The World Bank. https://www.gfdrr.org/sites/default/files/publication/The_Triple_Dividend_of_Resilience.pdf.

Tarozzi, A. and Deaton, A. (2009). Using Census and Survey Data to Estimate Poverty and Inequality for Small Areas. *The Review of Economics and Statistics* 91: 773–792, doi:10.2139/ssrn.997829.

Tesselaar, M., Wouter Botzen, W., Haer, T., Hudson, P., Tiggeloven, T. and Aerts, J. (2020). Regional inequalities in flood insurance affordability and uptake under climate change. *Sustainability* 12: 1–30, doi:10.3390/su12208734.

United Nations Framework Convention on Climate Change (2015). Paris Agreement.

Vousdoukas, M. I., Mentaschi, L., Voukouvalas, E., Verlaan, M., Jevrejeva, S., Jackson, L. P. and Feyen, L. (2018). Global probabilistic projections of extreme sea levels show intensification of coastal flood hazard. *Nature Communications* 9: 2360, doi:10.1038/s41467-018-04692-w.

Willner, S. N., Levermann, A., Zhao, F. and Frieler, K. (2018). Adaptation required to preserve future high-end river flood risk at present levels. *Science Advances* 4: eaao1914, doi:10.1126/sciadv.aao1914.

Winsemius, H. C., Jongman, B., Veldkamp, T. I. E., Hallegatte, S., Bangalore, M. and Ward, P. J. (2018). Disaster risk, climate change, and poverty: assessing the global exposure of poor people to floods and droughts. *Environment and Development Economics* 23: 328–348, doi:10.1017/S1355770X17000444.

Zabeo, A., Pizzol, L., Agostini, P., Critto, A., Giove, S. and Marcomini, A. (2011). Regional risk assessment for contaminated sites Part 1: Vulnerability assessment by multicriteria decision analysis. *Environment International* 37: 1295–1306, doi:10.1016/j.envint.2011.05.005.

724 Zhou, Q., Mikkelsen, P., Halsnæs, K. and Arnbjerg-Nielsen, K. (2012). Framework for economic pluvial flood risk assessment considering
725 climate change effects and adaptation benefits. *Journal of Hydrology* 414–415: 539–549, doi:10.1016/j.jhydrol.2011.11.031.

A Social weights

This section presents the distribution of the social weights derived in Equation 9 (Figure A1), and of the resulting flood risk measures of Equation 10 (Figure A2), for various dimensions of socioeconomic vulnerability and with the different values of the redistribution parameter e adopted throughout the analysis.

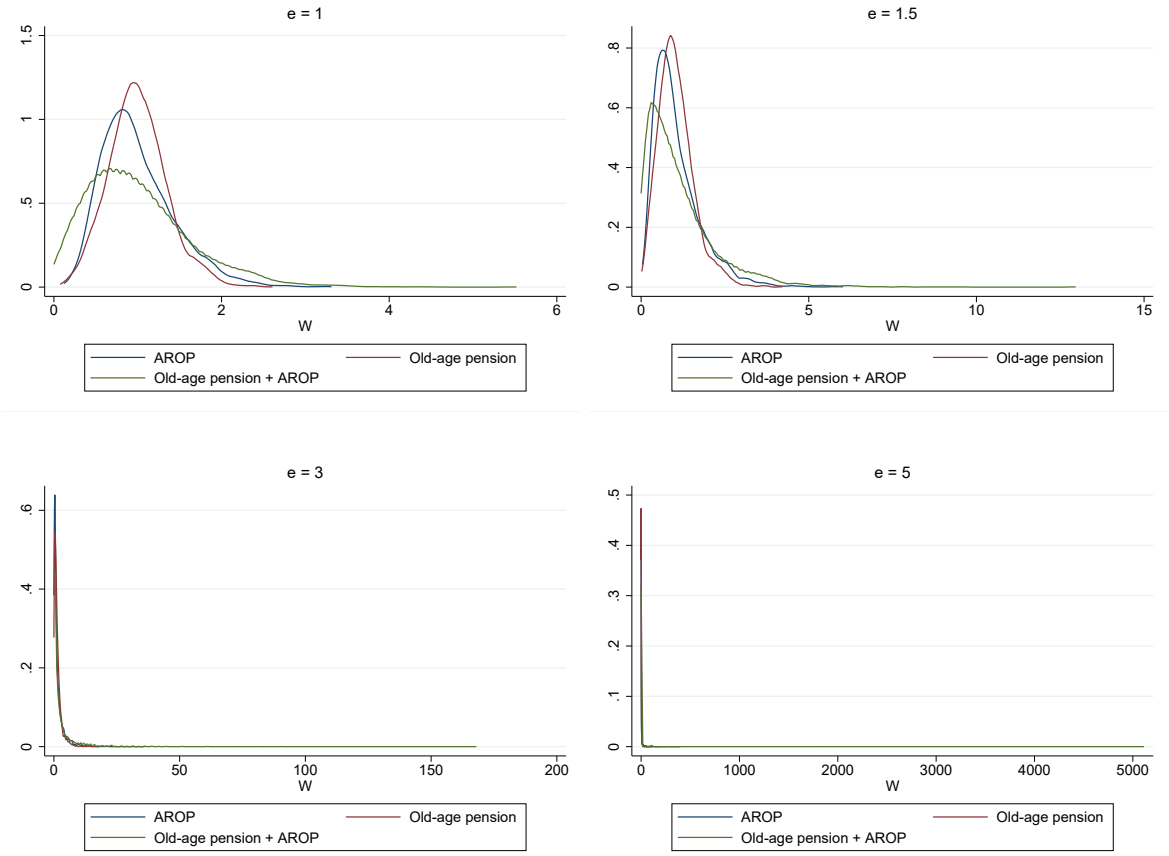

Figure A1: Social weights distribution

Notes: The figure displays the distribution of social weights from Equation 9 for various values of e. The social vulnerability measures are: the percentage of households in an electoral division that are at risk of poverty (AROP); the percentage of households in an electoral division that derive the majority of their income from old-age pension (Old-age pension); and the percentage of households in an electoral division that derive the majority of their income from old-age pension and are also at risk of poverty (Old-age pension + AROP).

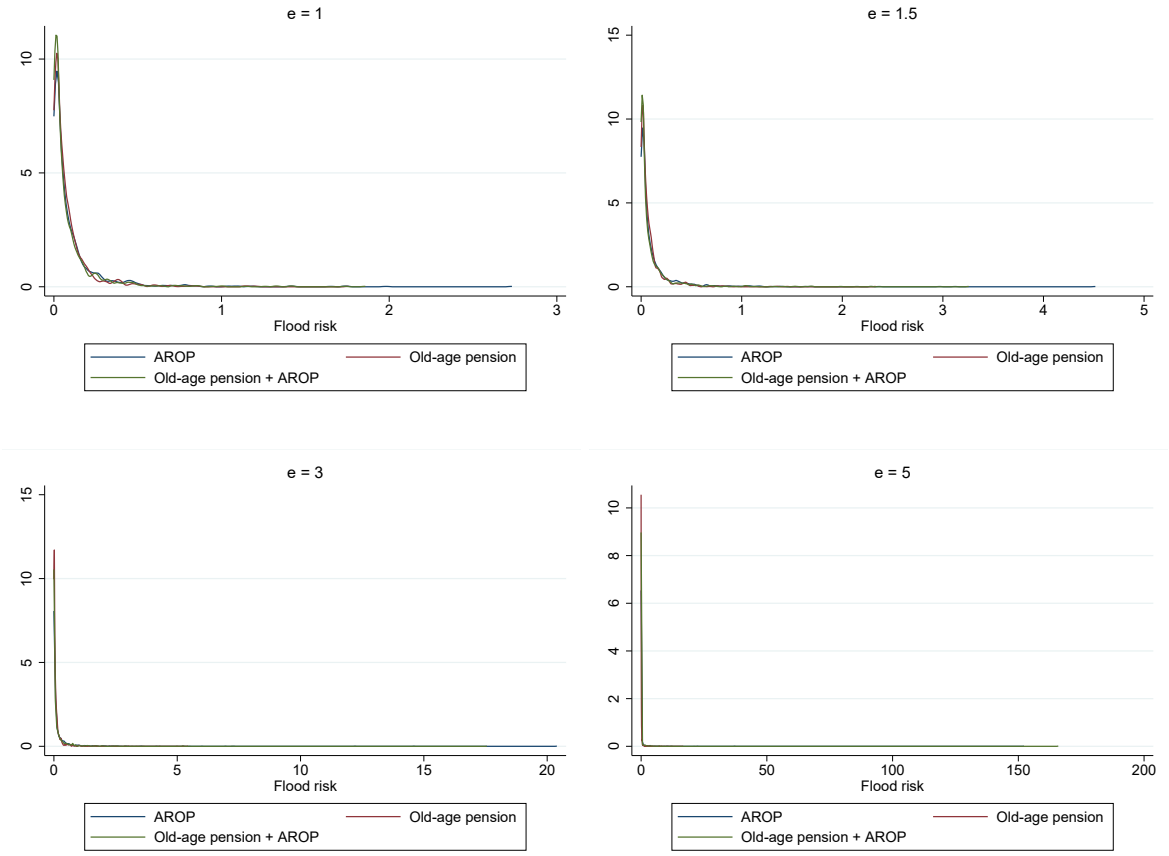

Figure A2: Flood risk distribution

Notes: The figure displays the distribution of flood risks from Equation 10 for various values of e in the social weight function. The social vulnerability measures are: the percentage of households in an electoral division that are at risk of poverty (AROP); the percentage of households in an electoral division that derive the majority of their income from old-age pension (Old-age pension); and the percentage of households in an electoral division that derive the majority of their income from old-age pension and are also at risk of poverty (Old-age pension AROP).

B Classification of flood hazard, exposure and risk

Table B1: Flood hazard natural breaks

	Lower bound	Upper bound	Size
No hazard	0	0	2,063
Very low hazard	2.2e-07	0.081431	831
Low hazard	0.082195	0.209583	321
Medium hazard	0.211146	0.391361	123
High hazard	0.398398	0.63778	47
Very high hazard	0.675216	1	24

Notes: This table displays the lower bound, upper bound and group size of the natural break classification for the flood hazard index reported in Equation 2.

Table B2: Top 20 electoral divisions by flood hazard

Electoral division	County	Province	% of area affected by flooding	H_n	MGI_n (€)	$MGI_n / \overline{MGI}$
Pembroke East C	Dublin City	Leinster	0.990	1	80,154	1.771
Pembroke East B	Dublin City	Leinster	0.987	0.998	76,865	1.698
John's A	Limerick City	Munster	0.976	0.987	24,527	0.542
North Dock A	Dublin City	Leinster	0.928	0.938	44,197	0.977
Dundalk No. 2 Urban	Co. Louth	Leinster	0.910	0.920	27,765	0.614
Ennis No. 3 Urban	Co. Clare	Munster	0.908	0.917	31,502	0.696
Dundalk No. 4 Urban	Co. Louth	Leinster	0.905	0.915	39,577	0.875
North Dock B	Dublin City	Leinster	0.874	0.883	56,062	1.239
Mansion House A	Dublin City	Leinster	0.830	0.839	35,885	0.793
Ballybough A	Dublin City	Leinster	0.815	0.823	31,504	0.696
Custom House	Limerick City	Munster	0.797	0.806	22,966	0.507
Limerick North Rural	Limerick City	Munster	0.795	0.804	42,394	0.937
Claddagh	Galway City	Connacht	0.787	0.796	41,294	0.912
John's B	Limerick City	Munster	0.776	0.784	23,601	0.521
Ballinacurra A	Limerick City	Munster	0.772	0.780	50,237	1.110
North Dock C	Dublin City	Leinster	0.768	0.776	48,549	1.073
Shannon A	Limerick City	Munster	0.763	0.771	37,257	0.823
John's C	Limerick City	Munster	0.741	0.749	30,089	0.665
Muckanagh	Co. Westmeath	Leinster	0.733	0.741	47,847	1.057
Dundalk No. 1 Urban	Co. Louth	Leinster	0.729	0.736	27,699	0.612

Notes: This table displays the top 20 electoral divisions according to their level of flood hazard reported in Equations 1 and 2. Column (6) reports the household median gross income in 2016, and Column (7) its ratio to the average household median gross income in Ireland for the same year. According to the CSO, the average household median gross income in Ireland in 2016 was €45,256.

Table B3: Flood exposure natural breaks

	Lower bound	Upper bound	Size
No exposure	0	0	2,067
Very low exposure	3.6e-06	0.063364	768
Low exposure	0.063692	0.168826	368
Medium exposure	0.170852	0.349739	133
High exposure	0.367115	0.650818	48
Very high exposure	0.674369	1	21
Removed	NA	NA	4

Notes: This table displays the lower bound, upper bound and group size of the natural break classification for the flood exposure index reported in Equation 5.

Table B4: Top 20 electoral divisions by flood exposure

Electoral division	County	Province	% of population affected by flooding	E_n	MGI_n (€)	$\text{MGI}_n / \overline{\text{MGI}}$
Pembroke East C	Dublin City	Leinster	1	1	80,154	1.771
Ennis No. 3 Urban	Co. Clare	Munster	1	1	31,502	0.696
Dundalk No. 4 Urban	Co. Louth	Leinster	1	1	39,577	0.875
John's A	Limerick City	Munster	1	1	24,527	0.542
Dundalk No. 2 Urban	Co. Louth	Leinster	0.996	0.996	27,765	0.614
North Dock C	Dublin City	Leinster	0.973	0.973	48,549	1.073
Pembroke East B	Dublin City	Leinster	0.969	0.969	76,865	1.698
Claddagh	Galway City	Connacht	0.911	0.911	41,294	0.912
Ballinacarrig	Co. Carlow	Leinster	0.892	0.892	54,663	1.208
Clontarf West D	Dublin City	Leinster	0.856	0.856	48,075	1.062
Ballybough A	Dublin City	Leinster	0.806	0.806	31,504	0.696
Ushers B	Dublin City	Leinster	0.805	0.805	38,143	0.843
John's B	Limerick City	Munster	0.797	0.797	23,601	0.521
Clenagh	Co. Clare	Munster	0.734	0.734	42,230	0.933
Graigue	Co. Laois	Leinster	0.717	0.717	47,533	1.050
Killukin	Co. Roscommon	Connacht	0.707	0.707	56,871	1.257
Dundalk No. 1 Urban	Co. Louth	Leinster	0.699	0.699	27,699	0.612
North Dock A	Dublin City	Leinster	0.698	0.698	44,197	0.977
North City	Dublin City	Leinster	0.680	0.680	44,053	0.973
Gurteen	Co. Waterford	Munster	0.675	0.675	49,319	1.090

Notes: This table displays the top 20 electoral divisions according to their level of flood hazard reported in Equations 4 and 5. Column (6) reports the household median gross income in 2016, and Column (7) its ratio to the average household median gross income in Ireland for the same year. According to the CSO, the average household median gross income in Ireland in 2016 was €45,256.

Table B5: Flood risk natural breaks — AROP

	Lower bound	Upper bound	Size
No risk	0	0	2,067
Very low risk	1.1e-06	0.035474	948
Low risk	0.035741	0.10508	281
Medium risk	0.106666	0.228676	76
High risk	0.234423	0.436813	26
Very high risk	0.51337	1	7
Removed	NA	NA	4

Notes: This table displays the lower bound, upper bound and group size of the natural break classification for the flood risk index reported in Equation 11, where the social vulnerability metric is the percentage of an electoral division's households at risk of poverty.

Table B6: Top 20 electoral divisions by flood risk — AROP

Electoral division	County	Province	Flood risk – weighted by % AROP	R_n	MGI_n (€)	$\text{MGI}_n / \overline{\text{MGI}}$
John's A	Limerick City	Munster	2.732	1	24,527	0.542
John's B	Limerick City	Munster	1.980	0.725	23,601	0.521
Abbey C	Limerick City	Munster	1.746	0.639	19,005	0.420
Dundalk No. 2 Urban	Co. Louth	Leinster	1.734	0.635	27,765	0.614
Ballybough A	Dublin City	Leinster	1.653	0.605	31,504	0.696
Custom House	Limerick City	Munster	1.427	0.522	22,966	0.507
North Dock C	Dublin City	Leinster	1.403	0.513	48,549	1.073
Dundalk No. 4 Urban	Co. Louth	Leinster	1.193	0.437	39,577	0.875
Ushers B	Dublin City	Leinster	1.166	0.427	38,143	0.843
Dundalk No. 1 Urban	Co. Louth	Leinster	1.096	0.401	27,699	0.612
Claddagh	Galway City	Connacht	1.094	0.400	41,294	0.912
Tralee Urban	Co. Kerry	Munster	1.051	0.385	23,021	0.509
Ennis No. 3 Urban	Co. Clare	Munster	1.036	0.379	31,502	0.696
Dundalk Rural	Co. Louth	Leinster	0.931	0.341	36,096	0.798
North City	Dublin City	Leinster	0.928	0.340	44,053	0.973
North Dock A	Dublin City	Leinster	0.859	0.315	44,197	0.977
Abbey B	Limerick City	Munster	0.839	0.307	40,010	0.884
Tumna North	Co. Roscommon	Connacht	0.835	0.306	29,452	0.651
Mountjoy A	Dublin City	Leinster	0.803	0.294	31,890	0.705
St. Nicholas	Galway City	Connacht	0.795	0.291	30,979	0.685

Notes: This table displays the top 20 electoral divisions according to their level of flood risk reported in Equations 10 and 11. The social vulnerability measure used to compute social weights is the percentage of electoral division's households at risk of poverty. Column (6) reports the household median gross income in 2016, and Column (7) its ratio to the average household median gross income in Ireland for the same year. According to the CSO, the average household median gross income in Ireland in 2016 was €45,256.

Table B7: Flood risk natural breaks — OAP

	Lower bound	Upper bound	Size
No risk	0	0	2,067
Very low risk	2.1e-06	0.048513	945
Low risk	0.049013	0.146723	308
Medium risk	0.14863	0.300699	65
High risk	0.329929	0.493007	15
Very high risk	0.647374	1	5
Removed	NA	NA	4

Notes: This table displays the lower bound, upper bound and group size of the natural break classification for the flood risk index reported in Equation 11, where the social vulnerability metric is the percentage of an electoral division's households deriving the majority of their income from old-age pension.

Table B8: Top 20 electoral divisions by flood risk — OAP

Electoral division	County	Province	Flood risk – weighted by % OAP	R_n	MGI_n (€)	$MGI_n / \overline{MGI}$
Ennis No. 3 Urban	Co. Clare	Munster	1.758	1	31,502	0.696
Dundalk No. 2 Urban	Co. Louth	Leinster	1.212	0.689	27,765	0.614
John's A	Limerick City	Munster	1.180	0.671	24,527	0.542
John's B	Limerick City	Munster	1.142	0.649	23,601	0.521
Dundalk No. 1 Urban	Co. Louth	Leinster	1.138	0.647	27,699	0.612
Dundalk No. 4 Urban	Co. Louth	Leinster	0.867	0.493	39,577	0.875
Tumna North	Co. Roscommon	Connacht	0.844	0.480	29,452	0.651
Graigue	Co. Laois	Leinster	0.820	0.467	47,533	1.050
Claddagh	Galway City	Connacht	0.806	0.459	41,294	0.912
Gurteen	Co. Waterford	Munster	0.768	0.437	49,319	1.090
Abbey C	Limerick City	Munster	0.713	0.406	19,005	0.420
Clontarf West D	Dublin City	Leinster	0.694	0.395	48,075	1.062
Ennismore	Co. Kerry	Munster	0.690	0.393	32,337	0.715
Moynsha	Co. Kerry	Munster	0.676	0.385	40,653	0.898
Ballinacurra B	Limerick City	Munster	0.632	0.359	35,197	0.778
Killukin	Co. Roscommon	Connacht	0.609	0.346	56,871	1.257
Clenagh	Co. Clare	Munster	0.605	0.344	42,230	0.933
Pembroke East B	Dublin City	Leinster	0.601	0.342	76,865	1.698
Lea	Co. Offaly	Leinster	0.588	0.334	43,061	0.951
Ballybough A	Dublin City	Leinster	0.580	0.330	31,504	0.696

Notes: This table displays the top 20 electoral divisions according to their level of flood risk reported in Equations 10 and 11. The social vulnerability measure used to compute social weights is the percentage of electoral division's households that derive the majority of their income from old-age pension. Column (6) reports the household median gross income in 2016, and Column (7) its ratio to the average household median gross income in Ireland for the same year. According to the CSO, the average household median gross income in Ireland in 2016 was €45,256.

Table B9: Flood risk natural breaks — OAP + AROP

	Lower bound	Upper bound	Size
No risk	0	0	2,067
Very low risk	0	0.039556	907
Low risk	0.039705	0.1123727	304
Medium risk	0.125733	0.288267	101
High risk	0.314442	0.539967	18
Very high risk	0.617191	1	8
Removed	NA	NA	4

Notes: This table displays the lower bound, upper bound and group size of the natural break classification for the flood risk index reported in Equation 11, where the social vulnerability metric is the percentage of an electoral division's households deriving the majority of their income from old-age pension and are also at risk of poverty.

Table B10: Top 20 electoral divisions by flood risk — OAP + AROP

Electoral division	County	Province	Flood risk – weighted by % OAP+AROP	R_n	MGI_n (€)	$\text{MGI}_n / \overline{\text{MGI}}$
Abbey C	Limerick City	Munster	1.857	1	19,005	0.420
Ennis No. 3 Urban	Co. Clare	Munster	1.734	0.934	31,502	0.696
Dundalk No. 4 Urban	Co. Louth	Leinster	1.419	0.764	39,577	0.875
Graigue	Co. Laois	Leinster	1.414	0.761	47,533	1.050
Dundalk No. 2 Urban	Co. Louth	Leinster	1.334	0.718	27,765	0.614
John's B	Limerick City	Munster	1.319	0.710	23,601	0.521
John's A	Limerick City	Munster	1.261	0.679	24,527	0.542
Clontarf West D	Dublin City	Leinster	1.146	0.617	48,075	1.062
Wexford No. 3 Urban	Co. Wexford	Leinster	1.003	0.540	25,017	0.553
Tralee Urban	Co. Kerry	Munster	1.003	0.540	23,021	0.509
Ballybough A	Dublin City	Leinster	0.954	0.513	31,504	0.696
Claddagh	Galway City	Connacht	0.862	0.464	41,294	0.912
Baldoyle	Fingal	Leinster	0.853	0.459	54,984	1.215
Kilberry	Co. Kildare	Leinster	0.844	0.455	42,139	0.931
John's C	Limerick City	Munster	0.810	0.436	30,089	0.665
Dundalk No. 3 Urban	Co. Louth	Leinster	0.773	0.416	31,059	0.686
North Dock C	Dublin City	Leinster	0.767	0.413	48,549	1.073
Ennis No. 1 Urban	Co. Clare	Munster	0.744	0.401	32,260	0.713
Tumna North	Co. Roscommon	Connacht	0.718	0.387	29,452	0.651
Dundalk No. 1 Urban	Co. Louth	Leinster	0.716	0.385	27,699	0.612

Notes: This table displays the top 20 electoral divisions according to their level of flood risk reported in Equations 10 and 11. The social vulnerability measure used to compute social weights is the percentage of electoral division's households that derive the majority of their income from old-age pension and are also at risk of poverty. Column (6) reports the household median gross income in 2016, and Column (7) its ratio to the average household median gross income in Ireland for the same year. According to the CSO, the average household median gross income in Ireland in 2016 was €45,256.